Journal of Magnetic Resonance 304 (2019) 16–34

Contents lists available at ScienceDirect

Journal of Magnetic Resonance

journal homepage: www.elsevier.com/locate/jmr

Perspectives in Magnetic Resonance

Experiments with direct detection of multiple FIDs

Ēriks Kupče [a,*], Kaustubh R. Mote [b], Perunthiruthy K. Madhu [b]

[a] Bruker UK Ltd., Banner Lane, Coventry CV4 9GH, United Kingdom
[b] TIFR Centre for Interdisciplinary Sciences, Tata Institute of Fundamental Research Hyderabad, 36/P Gopanpally Village, Ranga Reddy District, Hyderabad 500107, India

ARTICLE INFO

Article history:
Received 3 February 2019
Revised 26 March 2019
Accepted 29 April 2019
Available online 30 April 2019

Keywords:
Parallel NMR
Multiple receivers
Multi-FID detection
Interleaved acquisition
Parallel spectroscopy
Ultra-fast NMR
Hyperpolarization
Spatial encoding
NMR supersequences
Metabolomics
Solid-state NMR
Simultaneous cross-polarization
Afterglow magnetization
Residual polarization
Hadamard encoding
Reduced dimensionality
Multiplex phase cycling

ABSTRACT

Pulse schemes with direct observation of multiple free induction decays (FIDs) offer a dramatic increase in the spectral information content of NMR experiments and often yield substantial improvement in measurement sensitivity per unit time. Availability of multiple receivers on the state-of-the-art commercial spectrometers allows spectra from different nuclear species to be recorded in parallel routinely. Experiments with multi-FID detection have been designed with both, homonuclear and multinuclear acquisition. We provide a brief overview of such techniques designed for applications in liquid- and solid- state NMR as well as in hyperpolarized samples. Here we show how these techniques have led to design of experiments that allow structure elucidation of small molecules and resonance assignment in proteins from a single measurement. Probes with multiple RF micro-coils routed to multiple NMR receivers provide an alternative way of increasing the throughput of modern NMR systems. Solid-state NMR experiments have also benefited immensely from both parallel and simultaneous FID acquisition in a variety of multi-dimensional pulse schemes. We believe that multi-FID detection will become an essential component of the future NMR methodologies effectively increasing the information content of NMR experiments and reducing the cost of NMR analysis.

1. Introduction

Many new techniques have been proposed to speed up multi-dimensional NMR spectroscopy [1] – ultra fast NMR [2,3], fast pulsing techniques [4–8], non-conventional sampling techniques [9–17], parallel NMR [18,19], and hyper-dimensional NMR [20–23], to name a few. Each new development, however modest, becomes important if it complements other fast techniques. Experiments with direct multiple FID (Free Induction Decay) observation, either homonuclear [24,25] or multinuclear [19], deliver more information in a single measurement as compared to similar conventional experiments and in many cases offer higher sensitivity per unit time [26,27]. Here we provide a brief insight into different approaches and techniques used in experiments with multi-FID detection – the technique suitably termed MACSY (Multiple ACquisition SpectroscopY) [28]. We prefer the term 'multi-FID detection' rather than 'multi-FID acquisition' to avoid confusion with the data averaging techniques.

Many multi-FID detection (MFD) experiments are based on the use of multiple receivers. Utility of multiple receivers was first explored in MRI [29–32]. This led to development of the parallel MRI [33,34] that is based on the use of multiple surface coils tuned to the same nucleus (mostly, if not exclusively protons) providing increased sensitivity and faster image acquisition. The great success of parallel MRI has stimulated interest in potential applications of multiple receivers in NMR spectroscopy. The multi-receiver technology was gradually introduced in NMR [18,35] becoming a standard feature on the state-of-the-art NMR consoles in the last couple of years. However, unlike in MRI the multiple receiver NMR experiments are typically designed with multinuclear detection in mind, mainly because the commercially available NMR probes are designed to accommodate only one sample. Home-built probes housing multiple micro-coils [36] routed to multiple (^{1}H) receivers have been shown to greatly increase the throughput of NMR spectroscopy [37,38]. The availability of

* Corresponding author.
E-mail address: eriks.kupce@bruker.com (Ē. Kupče).

https://doi.org/10.1016/j.jmr.2019.04.018
1090-7807/

multiple receivers in the state-of-the-art systems is expected to further fuel the developments in this area.

2. Basic types of multi-FID detection experiments

2.1. Multinuclear detection schemes

The MFD experiments with multinuclear detection can be loosely categorized into three basic techniques – (i) parallel acquisition pulse schemes, (ii) pulse sequences with sequential data acquisition and (iii) interleaved experiments (see Fig. 1). A further classification into multinuclear and homonuclear detection experiments can be made within each of the three categories.

Compared to the conventional way of recording multi-dimensional NMR experiments (see Fig. 1a) the parallel acquisition technique offers significant time savings by detecting two or more FIDs simultaneously (in parallel, see Fig. 1b). By definition, the nuclear species that are observed simultaneously cannot be decoupled from each other. A significant advantage of this technique is that all spectra are recorded under exactly the same conditions. Therefore, the parallel acquisition technique is useful in spin systems where mutual coupling between the directly observed spins is negligible.

In the sequential MFD experiments (Fig. 1c) the magnetization that builds up in one experiment is stored (typically on a slowly relaxing nuclear species, such as ^{15}N or ^{13}C) and later used to acquire a different type of spectra. Alternatively, such magnetization can be refocused and re-used in a different type of experiment(s). In some instances it is possible to decouple the nuclear species that are observed sequentially.

Finally, the interleaved experiments (Fig. 1d) avoid disturbing passive spins in alternate experiments. Typically the experiment with direct detection of faster relaxing nuclei is placed into the recovery period of the experiment that detects slower relaxing nuclear species reducing the total acquisition time by approximately a factor of two or less. Depending on the relaxation properties, decoupling of the faster recovering spins may be possible [26]. If the relaxation properties of the two directly detected nuclear species are very different, several experiments involving fast relaxing nuclei may fit into the recovery period of experiments with direct detection of the slow relaxing nuclear species.

While many basic experiments nicely fit into one of these categories, more complex experiments often use mixed types of multiple FID detection. For instance, multinuclear detection can be combined with homonuclear multi-FID detection (HMFD) within the same experiment, as will be discussed in detail later. Likewise, experiments that include both, parallel and sequential data acquisition have been devised. A clear distinction should be made between acquiring spectra sequentially, which is the conventional way of recording NMR spectra (see Fig. 1a) and sequential acquisition of several FIDs in a single experiment (Fig. 1c) that typically involves detecting several coherence pathways in one experiment.

2.2. Homonuclear detection schemes and time-shared experiments

The homonuclear MFD experiments (HMFD) largely follow the same schemes as multinuclear MFD experiments (MMFD), except for the parallel acquisition experiments which require either multiple coil probes routed to multiple receivers [36,37] or some form of encoding, such as spatial or phase encoding. Parallel acquisition experiments based on phase encoding can be implemented on standard instrumentation and are better known as time-shared (*TS*) experiments [27]. For instance, simultaneous acquisition of ^{15}N-^{1}H and ^{13}C-^{1}H correlated experiments are typical examples of using the *TS* technique in practice [39–42]. Indeed, this technique is nowadays used routinely – suffice to mention IPAP methods delivering both In-Phase and Anti-Phase (IPAP) components [43–46], spectra simplification by 'virtual decoupling' [47,48] and many other experiments that involve the *TS* technique. Since this subject has been covered extensively in literature [27], we will only mention the *TS* technique where it has been incorporated into other MFD pulse schemes.

3. Multi-FID experiments in liquids

3.1. Multi-FID experiments with homonuclear (^{1}H) detection

There are many conceptual similarities between homonuclear and multinuclear MFD experiments. Indeed, some *sequential* acquisition multinuclear MFD experiments can be directly reproduced as homonuclear MFD experiments. For example, the COSY/HOESY experiment [26] is closely related to the COSY/NOESY (COCONOSY) pulse sequence [24,49]. Sequential acquisition is also employed in the NOAH (NMR by Ordered Acquisition using ^{1}H-detection) supersequences [25,50].

The parallel acquisition multinuclear MFD methods bear close similarity to the *TS* experiments. Accordingly, the *TS*-technique has similar limitations. For instance, the utility of simultaneous acquisition of the ^{1}H-^{13}C HSQC and ^{1}H-^{13}C HMBC in the *TS* fashion has been shown by several groups [51–54]. However, these *TS* pulse schemes do not permit ^{13}C decoupling in the HSQC spectra, which is straightforward in sequential detection mode [25]. The same applies to experiments involving broad-band homodecoupling [55].

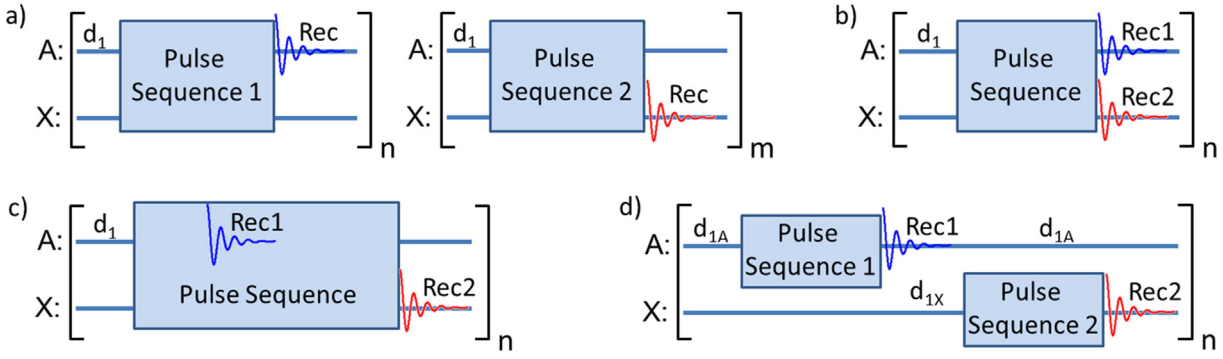

Fig. 1. Schematic representation of the basic types of multiple FID detection experiments where *n* and *m* are integers representing the number of increments in multi-dimensional NMR. A and X represent the observed nuclear species; (a) the conventional method of recording multi-dimensional NMR spectra sequentially; (b) parallel acquisition experiments; (c) sequential acquisition experiments and (d) interleaved experiments.

3.1.1. Early small molecule MFD experiments

The COCONOSY (COmbined COrrelated and Nuclear Overhauser enhancement SpectroscopY) experiment was the first multi-FID experiment recorded with homonuclear detection [24,49]. This experiment was subsequently reproduced also in solid-state NMR [56]. Two of the most useful H-H correlation techniques, the COSY and NOESY experiments are combined into a single experiment by recording the COSY spectrum during the NOESY mixing period, τ_{mix}:

$$(\pi/2)_{x,-x} - t_1 - (\pi/2)_x - acquire(\mathrm{COSY})_{x,-x}/t_{mix} - (\pi/2)_x - acquire(\mathrm{NOESY})_x$$

While the COSY experiment identifies proton spin systems via scalar H-H couplings, the NOESY experiment provides the distance information via through space (dipolar) interactions. Thus the combined information from these two experiments has been used for spectral assignment and structure elucidation of small proteins, such as BPTI in the early days of biomolecular NMR spectroscopy [57]. At that time it was not unusual for such experiments to take between 12 and 70 h of spectrometer time. In order to guarantee a perfect signal alignment the two spectra have to be recorded under identical and stable conditions. This can be a problem when dealing with unstable and degrading samples, as often is the case in biomolecular NMR. Not only the COCONOSY reduces the total experiment time to that of a NOESY experiment, but it also ensures that both spectra are recorded under identical conditions. Note, that the peak alignment in *F1* is guaranteed because in the COCONOSY pulse sequence both experiments share the same t_1 evolution period and therefore their spectral spaces share a joint *F1* frequency axis.

The combined 2D TOCSY/NOESY experiment proposed by Cavanagh and Rance exploits the same design principles [58]. The 2D TOCSY spectrum is recorded during the NOESY mixing period. Thus, both the 2D TOCSY and the 2D NOESY spectra are acquired in the same measurement time as that of a conventional 2D NOESY experiment.

Several combinations of the COSY/TOCSY experiment (abbreviated COTO) have been proposed by Parella et al. [59,60]. The variations include combinations with shared t_1 evolution period that are consistent with sequential acquisition schemes as well as experiments with separate t_1 evolution periods consistent with interleaved acquisition techniques. Schemes with interchanged TOCSY and COSY sequences, COSY/RELAY-3, TOCSY/TOCSY and COSY/TOCSY/TOCSY experiments with different TOCSY mixing times have been discussed [60,61].

The sequential acquisition technique combined with the *TS* method was used by Parella et al. to record multiple HMBC spectra in a single measurement [62]. The pulse sequence named MATS HMBC (Multiple Acquisition Time Shared HMBC) was used to simultaneously record up to four 2D spectra – H-C HMBC, H-N HMBC, H-C HMBC-COSY and H-N HMBC COSY. Both the HMBC and HMBC-COSY experiments share the t_1-evolution period ensuring perfect spectral alignment and facilitating peak assignment. The HMBC FID is recorded during the extended $^nJ(XH)$ (X = ^{13}C and ^{15}N) evolution period of the appended HMBC-COSY experiment emphasizing the long-range X-H correlations. Thus the experiment effectively records HMBC correlations with two settings of the *J*-evolution delays, one of which is also incremented with the t_1 period. This allows identifying correlations via up to seven bonds. The COSY type mixing can be replaced with the TOCSY mixing to produce the corresponding TOCSY versions of the experiment. The experiment time can be further reduced by using an Ernst angle (α) optimized excitation pulse. This technique has recently been further refined and extended also to HSQC/HSQC-TOCSY pulse schemes [59,61].

3.1.2. NOAH supersequences

The early HMFD experiments are based mainly on the PEP (Preservation of Equivalent coherence Pathways) principle [63]. This limits the number of experiments that can be combined into a single pulse scheme. The NOAH (NMR by Ordered Acquisition using ^{1}H-detection) experiments combine several techniques for multiple FID detection and take advantage of the presence of multiple isotopomers in diluted (natural abundance) spin systems allowing multiple complementary spectra to be recorded in a single experiment [25,50]. The NOAH supersequences are constructed by linking individual, specially adapted basic NMR sequences (modules) according to the domino principle – the tailored output of one module serves as an input for the following module (see Fig. 2a). Hence, a supersequence is defined as a sequence of such basic pulse sequences (modules). It has been shown that hundreds of NOAH-type supersequences can be constructed from the basic NMR sequences, such as 2D HMQC, HSQC, HMBC, COSY, DQF-COSY, NOESY and ROESY reformed as NOAH modules [25].

The recovery period, d_1 that is a basic component of essentially all NMR experiments is typically also by far the longest time period of most of the conventional NMR experiments [4–7]. The NOAH supersequences require only one recovery delay to record up to five or more spectra thus offering significant time savings which increase as more modules are combined into a single supersequence. In addition to the time savings the NOAH experiments benefit also from the fact that all spectra are recorded under identical conditions and in an identical experimental environment. This can be particularly beneficial when used in automated structure elucidation applications.

As an example, one such NOAH-4 supersequence consisting of four modules is shown in Fig. 2b. In this example the NOAH-4 experiment starts with the ^{15}N HMQC module that has been derived from the ASAP-HMQC pulse sequence [7]. The HMQC, rather than HSQC sequence, is chosen for recording the N-H correlation spectra because it manages the bulk magnetization more efficiently and typically the N-H multiplicity-editing is of little interest in small molecule NMR. The N-H HMQC module only uses the magnetization of protons directly bound to the ^{15}N nuclei, i.e. 0.36% of the total proton magnetization and the rest of the bulk

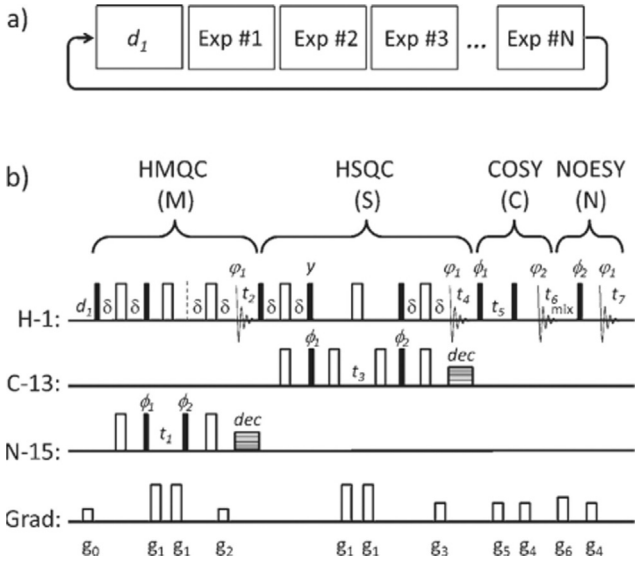

Fig. 2. (a) Assembling the NOAH modules into supersequences; only a single recovery delay (d_1) is employed; (b) the NOAH-4 MSCN supersequence consisting of four NOAH modules – ^{15}N HMQC (M), ^{13}C HSQC (S), COSY (C) and NOESY (N). Reproduced from [25] with permission.

magnetization (minus pulse imperfections) is kept along the Z axis for use in the following NOAH modules. The HMQC module (abbreviated by the letter *M*) is followed by the C-H HSQC module (abbreviated with the letter *S*) with optional multiplicity-editing. This module is derived from the ASAP-HSQC pulse sequence [8] and uses the magnetization of protons directly bound to the ^{13}C nuclei which constitutes 1.1% of the bulk proton magnetization. Rest of the bulk magnetization is aligned along the Z axis for most of the duration of the HSQC module, including the FID period. Finally, this NOAH-4 supersequence ends with COSY (C) and NOESY (N) modules derived from the COCONOSY experiment [24,49]. The spectra of cyclosporine recorded using a NOAH-5 (MSBCN) supersequence that includes also the HMBC module (B) are shown in Fig. 3.

While a large number of NOAH supersequences can be constructed from the basic modules, not all combinations are equally efficient and/or practical. For instance, the BC (HMBC/COSY) combination suffers from proton T_2 relaxation and diffusion losses.

In the NOAH-3 BSC supersequence (HMBC/HSQC/COSY) the B and S modules are interchanged by placing the less sensitive HMBC module before the HSQC module (see Fig. 4a). A ZZ-HMBC module that preserves the magnetization of protons directly bound to ^{13}C is introduced [50]. The bulk proton magnetization that is dephased by the coherence selection gradients of the ZZ-HMBC module partially recovers during the HMBC and HSQC acquisition periods and is used to record the COSY spectra. The ASAP-COSY module

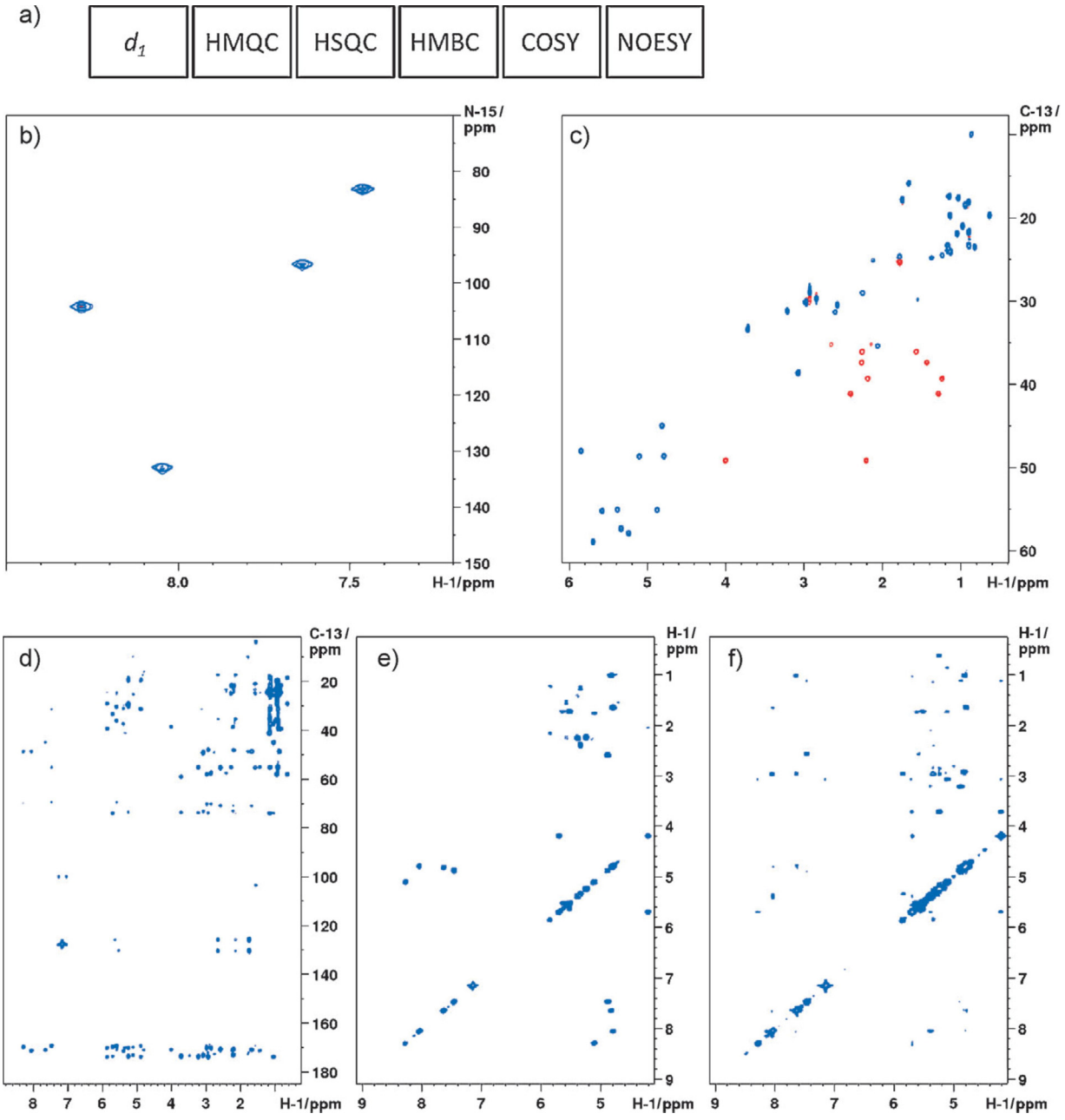

Fig. 3. (a) Order of the NOAH modules in the NOAH-5 MSBCN supersequence used to record five 2D spectra in a single measurement – (b) ^{15}N HMQC, (c) multiplicity-edited ^{13}C HSQC, (d) ^{13}C HMBC, (e) ^{1}H-^{1}H COSY and (f) ^{1}H-^{1}H NOESY; the sample is 50 mM cyclosporine in benzene-d_6; the spectra were recorded on AVANCE III spectrometer equipped with a TCI CryoProbe in 44 min with 2 scans per increment and 512 t_1-increments per module, resulting in a 2048 × 2560 raw data matrix. Reproduced from [25] with permission.

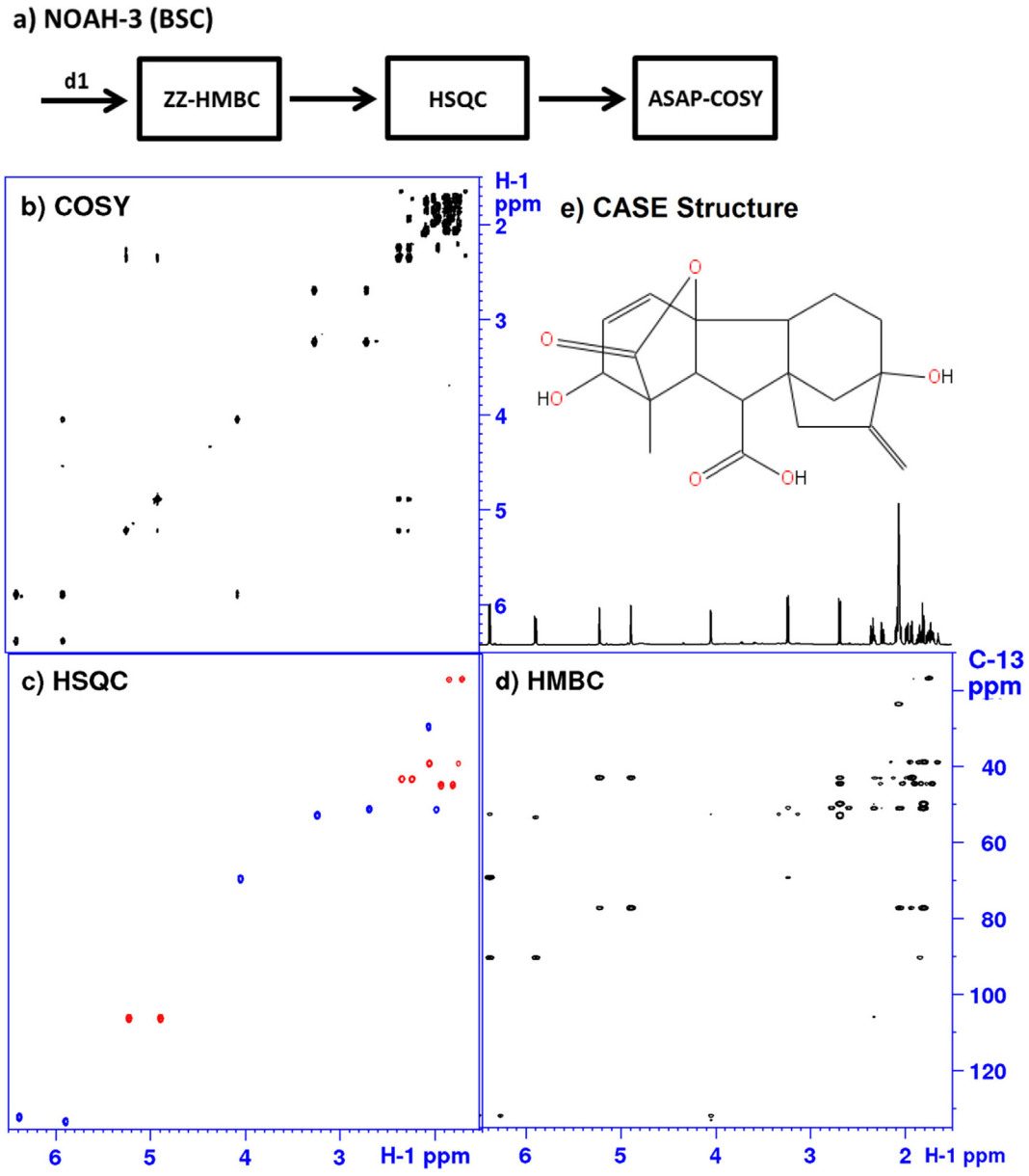

Fig. 4. (a) The NOAH-3 BSC supersequence consisting of the ZZ-HMBC (B), HSQC (S) and ASAP-COSY (C) modules; (b–d) the NOAH-3 BSC spectra recorded on a 700 MHz Bruker AVANCE III NMR spectrometer equipped with the TCI CryoProbe; (b) 2D H-H COSY, (c) multiplicity-edited 2D C-H HSQC and (d) 2D C-H HMBC spectra - all recorded in the same experiment; the sample is 10 mg of gibberellic acid in 500 ml of acetone d_6; (e) the highest ranked structure of the molecule generated by the Bruker CMCse structure elucidation software [73] based on spectra (b–d). Reproduced from Ref. [50] with permission.

is used to ensure more uniform COSY peak intensities. The NOAH-3 BSC supersequence proves to be a more robust experiment as compared to its SBC isomer. The NOAH-4 BSCN (HMBC/HSQC/COSY/NOESY) supersequence is constructed in a very similar way.

3.1.3. Molecular structure from a single NOAH supersequence

The possibility of structure elucidation of small molecules from a single measurement was initially demonstrated by the PANACEA experiment [64,65]. The MMFD based PANACEA pulse sequence relies on the ^{13}C–^{13}C INADEQUATE experiment [66–68] that provides unambiguous information about the C-C connectivities in the carbon skeleton of organic molecules but requires high sensitivity/high sample concentration or long acquisition times.

While the PANACEA experiment is uniquely positioned to analyse proton-deficient molecules, in more common situations structure of small organic molecules can also be established from three basic ^{1}H-detected 2D NMR experiments – HSQC, HMBC and COSY [69–73]. The HSQC, HMBC and COSY modules can be linked into several NOAH supersequences, such as NOAH-3 SBC, NOAH-3 BSC, NOAH-4 SBCN, NOAH-4 BSCN, NOAH-5 MSBCN and similar. Such supersequences provide all the information necessary for structure elucidation of small molecules in a single measurement (see Fig. 4). Moreover, the NOAH supersequences that include the NOESY (N) or ROESY (R) module additionally provide stereospecific information about the 3D structure of small molecules [50].

3.1.4. Biomolecular HMFD experiments

Several 3D experiments with sequential acquisition of pairs of ^{1}H detected 3D experiments based on the PEP principles [63] have been proposed by Ramachandran et al. [74,75]. Two pulse schemes – 3D HCCNH/HNCACONH and 3D HNCOCANH/HNCACONH, have been designed for protein backbone assignment from a single

measurement [75]. The methodology has been adapted from similar experiments in solids [76–78]. Typically the two experiments with different magnetization transfer pathways are started simultaneously and, at some point, the relevant ^{13}C or ^{15}N magnetization belonging to one of the pathways is kept in the z-state before the first data set is acquired. The stored magnetization is then used to complete the second pathway. Thus, the overall experimental time required to record the two 3D spectra is reduced by a factor of about two.

One important point to consider is that the duration of FIDs in solids is typically significantly shorter as compared to that in liquids. Consequently, the longer acquisition times in similar liquids experiments can introduce noticeable differential signal attenuation in larger proteins in the second data set depending on the duration of the acquisition time and variations in the Cα relaxation rates. Reduced acquisition times in the directly detected dimension combined with linear prediction improve the performance of the experiments [75].

The HNCACONH part of the sequential 3D HNCOCANH/HNCACONH experiment begins with $^{1}H_N$ magnetization that is transferred along the pathway $^{1}H_N(t_1)$ -> ^{15}N -> $^{13}C\alpha$ -> ^{13}CO -> ^{15}N (t_2) -> $^{1}H_N(t_3)$ of directly coupled nuclei. Simultaneously the 3D HCCNH part of the experiment starts from the side chain protons (^{1}Hsc) and follows a similar pathway $^{1}Hsc(t_1)$ -> ^{13}Csc -> $^{13}C\alpha$ -> $^{15}N(t_2)$ -> $^{1}H_N(t_3)$. When both the pathways cross at the $^{13}C\alpha$ site, part of the $^{13}C\alpha$ magnetization is stored in the *Z*-state while the other part is transferred to ^{15}N and then to $^{1}H_N$ for detection. This completes the HCCNH part of the sequence. Following the 3D HCCNH acquisition period the remaining $^{13}C\alpha$ magnetization is used to complete the 3D HNCACONH experiment. Provided that the amino acid type information is available from the conventional experiments e.g. CBCACONH the sequential 3D HNCACONH/HCCNH data set provides sufficient information for unambiguous sequential resonance assignment of the backbone ^{15}N and $^{1}H_N$ nuclei as well as the side chain protons. A similar approach is used in the sequential 3D HNCOCANH/HNCACONH pulse scheme [75] and experiments designed for medium size protein studies – 3D HA(CA)NH/HA(CACO)NH, 3D HA(CA)NH/H(N)CAHA and 3D H(N)CAHA/H(CC)NH [74].

3.2. Multinuclear detected multi-FID experiments

3.2.1. Small molecule experiments

Advent of multiple receiver technology in NMR enabled simultaneous observation of multiple nuclear species and greatly increased the number of potential applications of MFD experiments opening new avenues in NMR experiment design [79–81].

3.2.1.1. H-F COSY at Earth's magnetic field. At low magnetic fields, such as Earth's magnetic field, the resonance frequencies of various nuclear species become sufficiently close to allow simultaneous detection of resonances from several nuclei in the same spectrum. While at the Earth's magnetic field of ca 60 μT the homonuclear chemical shifts essentially disappear, the heteronuclear resonances are easily observed. Callaghan and co-workers have recorded 2D COSY spectra of fluorinated compounds, trifluoroethanol and para-difluorobenzene, showing the ^{1}H and ^{19}F diagonal peaks and the corresponding H-F cross-peaks in the same 2D spectrum [82].

3.2.1.2. Quadruple COSY with 4 receivers. As the magnetic field strength increases it becomes impossible to cover the resonance frequencies of several nuclear species with a single hard pulse simultaneously. The same is true for the tuning bandwidth of the NMR probes. However, modern multinuclear NMR probes can be tuned selectively and simultaneously to several nuclei. For instance, probes tuned to $^{1}H/^{13}C/^{15}N/^{31}P$ nuclei are routinely used in biomolecular applications. This allows applying pulses to several nuclear species simultaneously and on multi-receiver NMR systems also detecting the FIDs from several nuclear species simultaneously. Therefore, one way to record multinuclear correlation spectra is by multiplexing the conventional homonuclear pulse schemes. As an example, a 2D quadruple $^{1}H/^{13}C/^{15}N/^{31}P$ quadruple-COSY experiment has been recorded [80] wherein heteronuclear correlations appear as asymmetrically positioned peaks with intensities that depend on the gyromagnetic ratios, γ, of the indirectly detected (polarization source) nuclei. The ^{15}N cross-peaks were not observed in the spectra of high γ nuclei because of the inefficient polarization transfer from the low γ nuclei, ^{15}N. In practical applications the π/2 excitation pulses on low gamma nuclei may be omitted, leading to a simplified version of the quadruple-COSY, i.e. the PANSY (PArallel Nmr SpectroscopY) COSY pulse scheme [18].

3.2.1.3. H/C and H/C/N detected experiments – PANSY and PANACEA. Apart from a simple pulse and acquire experiment, one of the simplest *parallel acquisition* experiments is the simultaneous inversion-recovery T_1 relaxation measurement [26]. In this experiment both inversion-recovery pulse sequences are executed in parallel, but interleaved version of the experiment is also feasible. It should be noted that relaxation dynamics is slightly different in these two types of experiments. Generally, the PANSY experiments provide a different type of spectral information as compared to the interleaved experiments. Not all PANSY sequences can be converted into interleaved sequences and *vice versa*. Unlike the interleaved experiments, which typically can be just appended to each other, the parallel acquisition experiments usually have to be designed "from scratch" and typically involve a shared t_1-evolution, which guarantees a perfect peak alignment in the F1 dimension. Experiments that share one or more time domains belong to the same spectral space and therefore can also be seen as reduced dimensionality experiments [83].

Significant time savings in parallel acquisition experiments are achieved if polarization originates from high gamma and fast relaxing nuclei. Mutual decoupling of the directly observed nuclei during acquisition is generally not possible. Therefore, the parallel acquisition experiments are usually applied to spin systems with small and/or unresolved mutual *J*-couplings. Spectral simplification by various types of 'virtual' decoupling remains a possibility.

The PANSY COSY experiment [18] is probably one of the most versatile MMFD experiments, particularly in high gamma/high natural abundance combinations. The pulse scheme for the gradient version of the two-receiver experiment is shown in Fig. 5. It starts with a 90° pulse on the abundant (high γ, spin ½) nuclei, *A* (*A* = ^{1}H, ^{19}F, ^{31}P and alike) followed by the t_1-evolution period and simultaneous pulses on both, *A* and *X* nuclei (*X* = ^{1}H, ^{13}C, ^{15}N, ^{19}F, ^{29}Si, ^{31}P and alike) [79–81]. Note that in diluted spin systems (e.g. *X* = ^{13}C, ^{15}N, ^{29}Si) multiple COSY spectra originate from different molecules. In abundant spin systems a slightly different version of the PANSY-COSY pulse sequence with a reduced (45°) flip-angle ^{1}H read pulse may be used to avoid bleaching effects [26].

The sequential acquisition based TOCSY/HETCOR experiments designed for two receivers are shown in Fig. 6 [18,84]. In the 2D H-H TOCSY/1D X version of the experiment (see Fig. 6a) a simple pulse and acquire sequence is used to record a 1D X spectrum during the H-H mixing period. For instance, 1D ^{13}C spectrum can be recorded during the TOCSY mixing period (typically around 100 ms) which serves also as ^{1}H decoupling sequence for the 1D ^{13}C spectrum. 1D ^{13}C spectra are routinely recorded in small molecule NMR to obtain information about the number of ^{13}C atoms in the molecule and to obtain preliminary information about the spectral windows of interest for the subsequent HSQC and HMBC

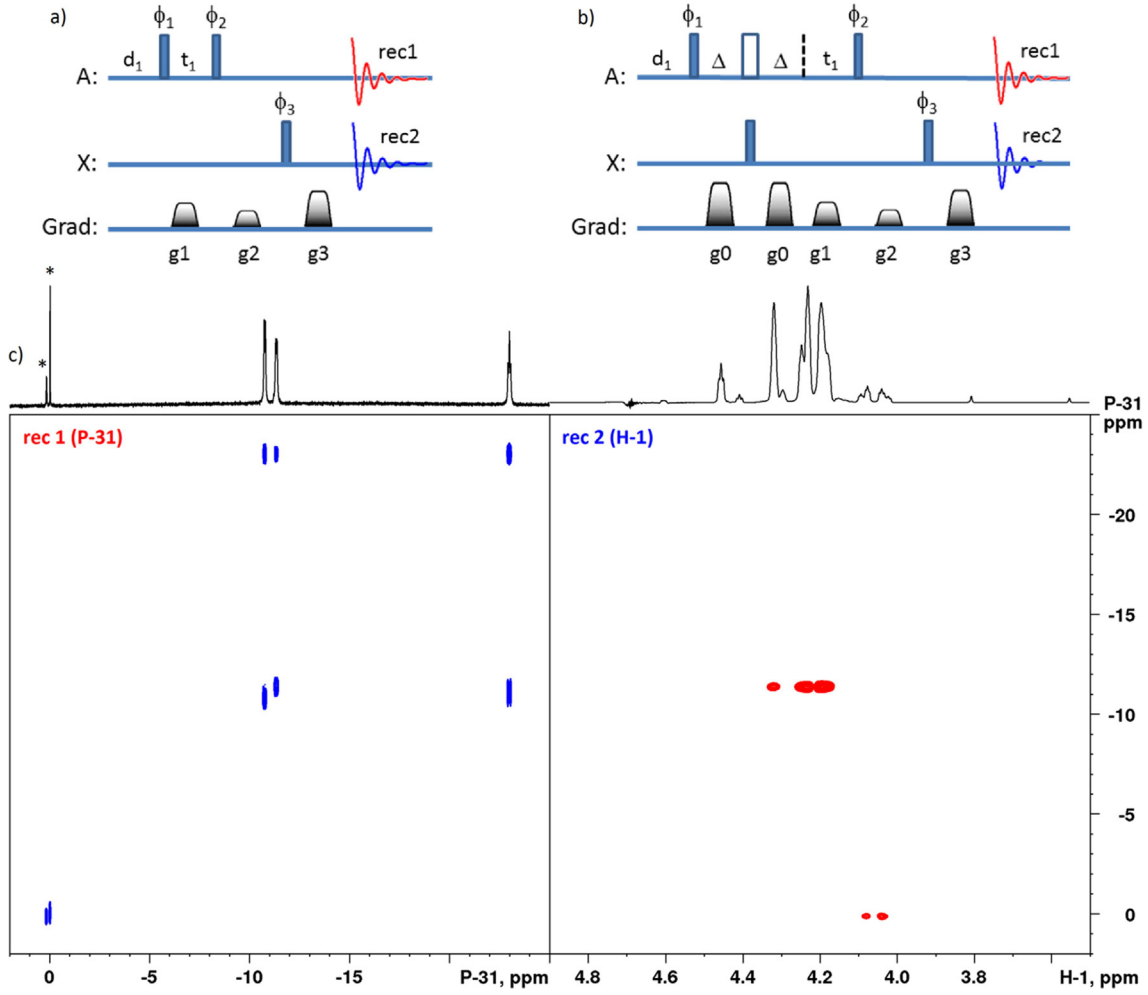

Fig. 5. The dual receiver PANSY-COSY experiment; (a) the basic pulse sequence; (b) the pulse scheme with suppression of one-bond A-X (^{1}H-^{13}C) correlations; (c) the P/H PANSY-COSY spectra of ATP in D_2O recorded on a Bruker Avance III HD spectrometer operating at 700 MHz (^{1}H) frequency. Minor impurities (AMP and ionic phosphate) are marked by asterisks.

experiments. Such information is crucial also for fast NMR techniques such as Hadamard NMR [13,84], ultrafast NMR [2,3] and spectral folding [85].

The 2D TOCSY/HETCOR version of the experiment (see Fig. 6b) begins with the refocused INEPT sequence. At the end of the INEPT transfer the bulk proton magnetization is preserved and aligned with the *Z* axis together with the polarized *X* spin magnetization. Following a purge gradient and the *X* read pulse the TOCSY mixing is switched on. The H-X HETCOR spectrum with optional multiplicity-editing is recorded during the TOCSY mixing period. After the H-H mixing period the HETCOR experiment is completed and another purge gradient is applied before a ^{1}H read pulse is followed by the 2D H-H TOCSY acquisition period.

Other modifications of this experiment include the 2D TOCSY/HETCOR-Q experiment that acquires 2D H-H TOCSY, 2D H-C HETCOR and 1D ^{13}C spectrum of non-protonated carbon sites in a time-shared manner [84]. The same paper describes the Hadamard version of the 2D TOCSY/HETCOR experiment for fast acquisition of the H-H TOCSY and H-C HETCOR (see also the supporting information in [18]).

The PANACEA pulse scheme allows structure elucidation of small molecules from a single measurement [64,65,86]. In its basic configuration the PANACEA experiment provides 2D C-C INADEQUATE, H-C HSQC and H-C HMBC spectra in a single pass. The C-C INADEQUATE pulse sequence [66–68] is one of the most powerful tools for structure elucidation of small molecules, but suffers from low sensitivity. Therefore the PANACEA experiment starts with the ^{13}C detected 2D C-C INADEQUATE sequence that runs for the whole duration of the PANACEA experiment. At the same time different variations of the 2D H-C HSQC and 2D HMBC or 3D *J*-HMBC are recorded sequentially. These ^{1}H-detected experiments utilize the bulk single quantum (SQ) ^{13}C magnetization that is suppressed in the conventional INADEQUATE experiments. This SQ ^{13}C magnetization is frequency encoded and transferred to protons for detection.

A minor phase cycle modification in the INADEQUATE sequence allows recording the 1D ^{13}C spectra in parallel with the 2D INADEQUATE spectra in a *TS* manner. In addition to providing the total number of the ^{13}C atoms in the molecules the 1D ^{13}C spectra can be used for field/frequency correction of all PANACEA spectra thus replacing the conventional deuterium field/frequency lock. This allows recording the PANACEA spectra in neat liquids [65].

The three versions of the 2D H-C HSQC spectra can be recorded by incrementing the t_4 delay in steps of $0.25/^{1}J(CH)$. This generates spectra with (a) all peaks positive, (b) positive CH and CH_3 and negative CH_2 signals and (d) CH and CH_3 peaks only providing an extra dimension for further resolution improvement in crowded HSQC spectra of molecules such as toxins and small peptides.

Once the 2D HSQC spectra have been collected the ^{13}C decoupling is switched off and the t_4 delay is set for recording the H-C

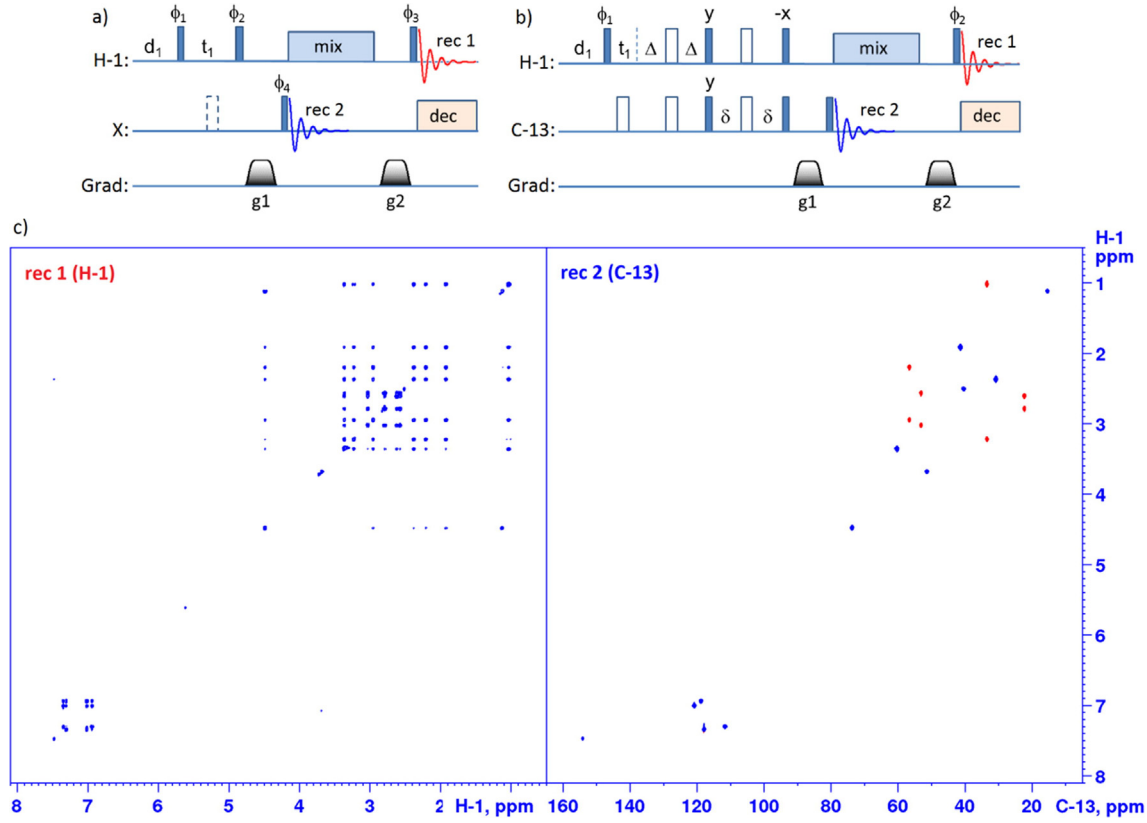

Fig. 6. (a) The dual-receiver pulse scheme for recording 2D H-H TOCSY/1D X spectra. The dotted rectangle represents an optional π(X) pulse for abundant X spins [26]; (b) the 2D H-H TOCSY/H-X HETCOR pulse scheme (c) the 2D TOCSY (receiver 1) and 2D multiplicity-edited H-C HETCOR (receiver 2) spectra of ajmalicine in DMSO d_6 (10 mg/600 µl) recorded on a Bruker Avance NEO 800 MHz instrument in 12 min using the pulse sequence (b); 256 increments, 2 scans per increment; the negative CH_2 peaks in the HETCOR spectra are shown in red; the positive (CH and CH_3) peaks are shown in blue. (For interpretation of the references to colour in this figure legend, the reader is referred to the web version of this article.)

HMBC spectra. In order to cover all the $^{n}J(CH)$ couplings of interest several 2D H-C HMBC spectra with different t_4 delay settings can be recorded. Alternatively, the t_4 delay can be incremented systematically to produce a 3D *J*-HMBC spectrum. The long range C-H couplings can be extracted from the HMBC spectra with high accuracy providing further stereospecific information about the 3D structure of the molecules [86]. Since the total duration of the PANACEA experiment is determined by the sensitivity of the INADEQUATE part, the number of the additional HMBC and HSQC spectra can be adjusted accordingly. In high concentration/high sensitivity samples the PANACEA spectra have been recorded in as little as 23 min [65].

The INEPT polarization transfer can be used to enhance the sensitivity of the INADEQUATE step in situations with no or very few of non-protonated carbon or other hetero-atom sites. For instance, the INEPT-INADEQUATE combination has been used for recording the 2D Si-Si INADEQUATE based PANACEA experiments in silicon oils [87].

3.2.1.4. H/F detected experiments. High natural abundance, large chemical-shift range, and NMR sensitivity that is inferior only to that of protons but also because of a large chemical-shift range and excellent signal dispersion make fluorine-19 a very popular NMR nucleus [88–91]. High sensitivity of the ^{19}F nuclei to local electronic environment makes ^{19}F NMR an increasingly popular tool for the fragment-based drug design [90]. ^{19}F NMR plays an important role in the drug discovery methodology and in the pharmaceutical industry in general.

The *interleaved* H-H and F-F COSY experiments [26,92] are based on the standard COSY sequences that are recorded during the recovery period of the alternative nuclear species as schematically shown in Fig. 1d. The excitation pulses are applied in the individual experiments exclusively to one type of nuclear species while the other nuclear species are left unperturbed. Consequently, the strength of the gradient pulses can be set independently in the two interleaved experiments. The repetition time in the interleaved experiments is determined by the longest relaxing nuclear species, typically ^{1}H in this case. Significant contributions from the chemical-shift anisotropy (CSA) mechanism can substantially reduce ^{19}F T_1 relaxation time in asymmetric environments [91]. This often means that ^{19}F decoupling is possible in the interleaved H/F experiments because there is ample time for the ^{19}F nuclei to recover before the ^{19}F detected part of the experiment.

The interleaved H-C and F-C HMQC experiments can be recorded in a very similar fashion [26]. Once again ^{19}F decoupling can be used in the H-C HMQC part of the experiment provided $T_1(^{19}F) << T_1(^{1}H)$. In samples where the two recovery times are comparable ^{19}F decoupling must be omitted otherwise the speed advantage is lost. Note that in practice the order of the two pulse sequences does not matter because the experiment is *cyclic*. An important advantage of the interleaved experiments is that the offset and the spectral width in the indirect (^{13}C) dimension can be set independently for the ^{1}H and ^{19}F HMQC segments of the experiment.

Examples involving ^{1}H and ^{19}F direct detection demonstrate the great flexibility of this technique, particularly in situations involving nuclei with high sensitivity and high natural abundance. Many other experiments such as TOCSY, NOESY, DQ COSY, HSQC, HMBC and similar can be recorded as interleaved experiments. For instance, interleaved H/F 2D DOSY experiments have been

reported [26]. Combining different pulse sequences with direct ^{1}H- and ^{19}F-detection is also feasible.

While the interleaved experiments offer great flexibility and simple pulse scheme designs the speed advantages are usually greater in the parallel acquisition experiments [26]. The parallel H/F PANSY-COSY experiment records H-H COSY and H-F COSY while parallel F/H PANSY-COSY produces F-F COSY and F-H COSY spectra. Typically the ^{19}F bandwidth is much broader as compared to the ^{1}H bandwidth. Therefore, it can be advantageous to have ^{1}H in the indirectly detected joint F1 dimension. On the other hand, the ^{19}F recovery times are much shorter since typically $T_1(^{19}F) < T_1(^{1}H)$. Therefore the F/H PANSY-COSY experiment requires shorter repetition times. Wider ^{19}F bandwidth as compared to the ^{1}H bandwidth means that more t_1-increments are generally required to achieve a similar spectral resolution. Hadamard encoding [13] can be used to circumvent the problem. For example, the Hadamard version of the F/H PANSY-COSY experiment takes advantage of the shorter ^{19}F relaxation times producing the F-F COSY and F-H COSY spectra in just 3 s compared to 3 min required for the same experiment using the conventional sampling.

Both ^{1}H and ^{19}F are high sensitivity nuclei that can be used in parallel for indirect detection of low sensitivity, low gamma nuclei [93]. For example, in the PANSY H/F-C HSQC pulse sequence the two HSQC sequences are executed in parallel. The technique bears close resemblance to the *TS* approach, but does not require phase encoding for separating the simultaneously acquired spectra. The INEPT delays in the two sub-sequences are adjusted to account for the differences in the $^{1}J(HC)$ and $^{1}J(FC)$ couplings. In this case the repetition rate of the experiment is determined by the longest relaxation rate of the two types of the high gamma nuclei, which usually is ^{1}H.

The H/F-X (X = ^{13}C or ^{15}N) PANSY-HMBC experiment employs coherence selection gradients. To account for the different gyromagnetic ratios of ^{1}H and ^{19}F nuclei a proton refocusing pulse and a balancing gradient pulse is applied just before the parallel acquisition stage. Thus the protons are experiencing the difference between the two gradients while ^{19}F nuclei are affected by sum of the last two gradient pulses. In order to account for the differences in the $^{1}J(HC)$ and $^{1}J(FC)$ couplings in the corresponding ^{1}J-filters the starting point of the F-C HMBC pulse sequence is slightly delayed. The $^{1}J(FN)$ filter is usually not required for the H/F-N PANSY HMBC providing more flexibility in setting the ^{n}J-evolution delays. The two 2D H-C and F-C HMBC (and HSQC) spectra share the ^{13}C frequency axis. Thus, these experiments essentially provide three-dimensional H-F-C correlation information and can be thought of as reduced dimensionality experiments.

Just like the parallel acquisition experiments the *sequential acquisition* experiments typically involve shared coherence transfer pathways and the associated t_1-evolution period(s), except the sequential acquisition experiments take advantage of long *J*-evolution delays or other coherence transfer periods, such as TOCSY and NOESY mixing periods to acquire additional spectra 'as soon as possible' (see Fig. 1c). This is a crucial difference from the parallel acquisition experiments because it enables mutual decoupling of the directly detected nuclei.

The 2D dual receiver COSY/HOESY experiment [26] involves *sequential acquisition* and can be seen as a heteronuclear version of the COCONOSY experiment [24,49]. The pulse sequence incorporates a joint ^{1}H evolution period and ^{1}H decoupling during the ^{19}F (H-F HOESY) acquisition period. The ^{1}H FID of the H-H COSY experiment is recorded during the HOESY mixing time and does not contribute to the total duration of the H-F HOESY experiment.

3.2.2. Biomolecular MMFD experiments

In biomolecular research, there is considerable interest in direct detection of the low-γ nuclei, such as ^{15}N or ^{13}C, partly because they are less susceptible than protons to broadening by paramagnetic species [94]. The dramatic increase in sensitivity of direct observation of low-gamma nuclei in the last decade offered by cryogenic probe technology coupled with multiple receiver availability on the latest generation commercial spectrometers makes direct detection of low-γ nuclei suitable for multinuclear MFD experiments.

In biomolecular NMR the samples are typically enriched in ^{13}C and ^{15}N isotopes. Therefore the MMFD experiments are typically based on the PEP principles [63]. In the conventional bioNMR experiments the magnetization usually diverges into several coherence pathways and typically only one of the pathways leads to the desired multi-dimensional spectrum. Multiple receivers make it possible to observe simultaneously coherences from several coherence pathways in the same experiment. Such experiments provide more information in a single measurement as compared to conventional experiments recorded with a single receiver.

3.2.2.1. Experiments with sequential acquisition – Making use of the 'afterglow'. A significant advantage of the sequential acquisition experiments is that mutual decoupling of the directly observed nuclei is feasible. For sensitivity reasons it is beneficial to start sequential MMFD experiments with detection of the least sensitive nuclear species (e.g. ^{15}N), and then transfer the remaining magnetization to a more sensitive species (e.g. ^{13}C) for further detection finishing the experiment on the most sensitive nuclei, typically ^{1}H. As an example, consider the ^{13}C-detected two-dimensional 2D (HA)CACO experiment that correlates the Cα and CO chemical shifts in F1 and F2, respectively [95]. By using ^{13}CO detection this experiment can be recorded simultaneously with a 3D ^{1}H-detected (HA)CA(CO)NNH experiment [96]. The combined 2D (HA)CACO (black)/3D (HA)CA(CO)NNH experiment starts with ^{13}C detected 2D (HA)CACO pulse sequence. The residual ^{13}C magnetization ("afterglow") left over after the (HA)CACO experiment has decayed too far for direct ^{13}C detection. However, in this dual receiver experiment it is refocused, and transferred to protons for detection taking the advantage of higher proton sensitivity. Thus ca 10% of the ^{13}C signal originating on CO at the start of the ^{13}C detected 2D (HA)CACO acquisition, is used to record 3D (HA)CA(CO)NNH experiment with essentially no penalty in spectrometer time.

The magnetization flow during the 2D (HA)CACO/3D (HA)CA (CO)NNH experiment is summarized as follows:

$$H\alpha \overset{J_{HC}}{\rightarrow} C\alpha, t_1 \overset{J_{C\alpha CO}}{\rightarrow} CO, t_2$$

$$H\alpha \overset{J_{HC}}{\rightarrow} C\alpha, t_1 \overset{J_{C\alpha CO}}{\rightarrow} CO \overset{J_{CON}}{\rightarrow} N, t_2 \overset{J_{HN}}{\rightarrow} H^N, t_3$$

Note that the 3D experiment shares the first t_1 (Cα) evolution period with the 2D data set.

In samples not limited by sensitivity the speed of the measurements is further increased using the projection-reconstruction (PR) technique [15,97,98]. The PR experiment employed 56 increments in the jointly sampled time dimension and was completed in 15 min. The experiment is expected to have utility for small to moderately sized proteins (<50 kDa) as well as for intrinsically disordered proteins.

A conceptually similar experiment for simultaneous acquisition of ^{13}Cα–^{15}N and ^{1}H–^{15}N–^{15}N sequential correlations in proteins has been reported by Hosur, *et al.* [35]. The 3D HNN pulse sequence is modified to allow for multinuclear detection involving two receivers. In this experiment it is the ^{13}Cα magnetization that is utilized to record sequential ^{13}Cα–^{15}N correlations along with the standard 3D ^{15}N–^{15}N–^{1}H correlation spectra thus providing directionality to sequential walk in the 3D HNN spectra and facilitating the protein backbone assignment. The magnetization that in the conventional

3D HNN experiment is destroyed by gradients is detected in the second receiver to produce the 2D N-Cα correlation spectrum. This is followed by a second ^{15}N constant time evolution and INEPT transfer of the ^{15}N magnetization back to the amide protons for detection. Below the magnetization transfer pathways for the entire experiment are summarized:

$$H_i \rightarrow N_i, t_1 \rightarrow C_i^{\alpha}, C_{i-1}^{\alpha}, t_2^{'} \rightarrow N_i, N_{i-1}, N_{i+1}, t_2 \rightarrow H_i, H_{i-1}, H_{i+1}, t_3$$

The 2D ^{13}Cα–^{15}N correlation spectrum provides sequential connectivity between consecutive residues $i-1$, while the HNN spectrum reveals ^{1}H$_N$ and ^{15}N correlations between three consecutive residues, $i-1$, i, and $i+1$. The experiment provided complete assignment of resonances for a protein sample (ubiquitin) in a single measurement.

3.2.2.2. Pulse schemes with parallel detection. One drawback of the sequential acquisition experiments is that the direct detection periods that are within the pulse scheme, rather than at the end, are usually restricted in length, limiting the available resolution. This problem can be overcome by parallel acquisition of signals from distinct coherence pathways so long as the observed nuclei are not scalar coupled or the mutual scalar couplings are small and remain unresolved. As a practical example, consider the ^{15}N HSQC and HNCA pulse sequences (Fig. 7a) with parallel ^{1}H$_N$ and ^{13}CO acquisition [83]. The two-bond scalar couplings between ^{1}H$_N$ and ^{13}CO nuclei are small (<5 Hz) and usually remain unresolved, so that mutual decoupling of these nuclei is not essential and parallel acquisition can be used. The experiments start with INEPT transfer from protons to ^{15}N. During the subsequent period nitrogen transverse magnetization evolves with respect to the one-bond $^{1}J_{NCO}$ and $^{1}J_{NH}$ scalar couplings and ^{15}N chemical shift. Each of the two components, N_Z and $2N_ZCO_Z$, subsequently follows separate pathways *en-route* to detection. The $^{1}J(C',N)$ evolution period, T_N is chosen such that the cosine and sine terms are approximately 0.174 and 0.985, respectively, thus balancing the sensitivity of the ^{1}H and ^{13}C detected spectra. This can be optimized on a case by case basis. The $^{1}J(^{13}CO,^{13}C\alpha)$ scalar coupling is suppressed using the IPAP scheme [43–46].

The 2D ^{1}H/^{13}CO-detected ^{15}N HSQC experiment provides resonance frequencies of three nuclei, ^{13}CO, ^{15}N and ^{1}H$_N$, as in the 3D HNCO experiment [95]. The two data sets share the t_1 (^{15}N) evolu-

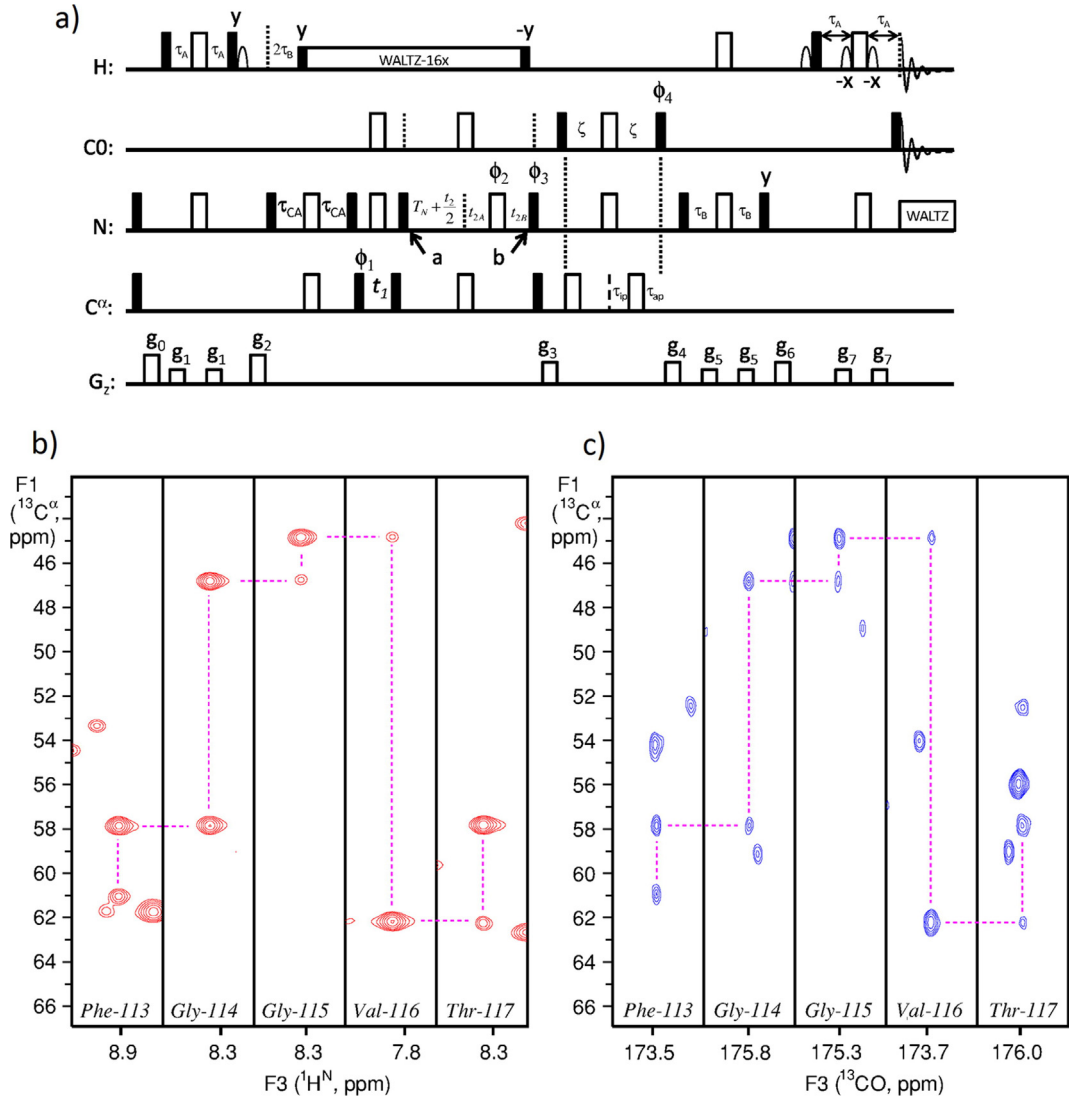

Fig. 7. (a) The pulse scheme for dual receiver ^{1}H/^{13}CO-detected HNCA experiment and F1F3 strip plots of (b) ^{1}H$_N$- and (c) ^{13}CO-detect 3D HNCA spectra of the Lb-FABP protein (the chicken liver fatty acid binding protein, Asla Biotech, 1 mM in 9:1 H2O/D2O, 25° C) recorded on an Agilent 18.8 T DDR2 NMR system equipped with two receivers and a cryogenic ^{13}C and ^{1}H enhanced sensitivity probe. The $^{1}J_{C\alpha CO}$ coupling was suppressed using the IPAP scheme. The total experiment time was 11 h 20 min. Reproduced from [83] with permission.

tion period and the F1 frequency axis and are equivalent to the orthogonal ^{15}N–^{13}CO and ^{15}N–$^{1}H_N$ projections of the 3D HNCO experiment from which the 3D HNCO spectrum can be reconstructed. Not only the two data sets recorded in parallel provide complementary information, but they also help to resolve ambiguities caused by signal overlap in similar with the 3D HNCO experiment.

The approach for designing the parallel 2D $^{1}H/^{13}CO$-detected ^{15}N HSQC experiment can be expanded to 3D and higher dimensionality experiments. For instance a parallel $^{1}H/^{13}CO$-detected 3D HNCA pulse scheme similar to the conventional HNCA pulse sequence [95] has been proposed (see Fig. 7a) [83]. A pair of 3D data sets correlating $^{13}C\alpha$ – ^{15}N – $^{1}H_N$ and $^{13}C\alpha$ – ^{15}N – ^{13}CO are obtained in a single measurement. The two 3D data sets share two indirect evolution periods, t_1 and t_2 and therefore a joint F1F2 plane ($^{13}C\alpha$, ^{15}N). Thus the experiment provides information about four nuclei, $^{1}H_N$, ^{15}N, $^{13}C\alpha$ and ^{13}CO and can be regarded as a reduced dimensionality 4D HNCACO experiment.

Fig. 7b and c compare strip plots from the pair of parallel $^{1}H/^{13}CO$-detected 3D HNCA data sets. High quality data sets of Lb-FABP protein (125 residues) were obtained, with 119 intra- and inter-residue correlations and 116 intra-, 109 inter-residue cross-peaks observed in the $^{1}H_N$ and ^{13}CO detect experiments, respectively (out of a possible 122). A comparison of both data sets makes it very easy to link $^{1}H_N$ and ^{13}CO chemical shifts and because the ^{13}CO chemical shift is recorded directly much higher resolution can be obtained than from conventional HNCO data sets. This demonstrates the feasibility to obtain the backbone assignment of small to medium size proteins from a single 3D measurement.

An alternative scheme for backbone assignment from a single experiment with magnetization originating from $^{1}H\alpha$ has been proposed by Reddy and Hosur [99]. The magnetization transfer pathways for this experiment are summarized below (Scheme 1):

Following the $^{1}H\alpha$ evolution the proton magnetization is transferred to $C\alpha$ where it is split into two pathways – part of magnetization is transferred to ^{15}N nuclei and the other part remains on the $C\alpha$ nuclei. In similar with the dual receiver HNCA experiment [83] this step is used to balance the sensitivities of the ^{1}H and ^{13}C detected spectra of this HA(CA)NH/HACACO experiment. Following two independent evolution periods (t_2 and t'_2) the magnetization is transferred to ^{1}H and ^{13}CO for detection. Thus, two 3D experiments - HA(CA)NH and HACACO with a joint $^{1}H\alpha$ frequency axis are recorded in parallel. This experiment involves five evolution periods and therefore can be regarded as a reduced dimensionality (5D/3D) experiment. To further facilitate the resonance assignments the pulse sequence has been extended to parallel 3D HBHA(CA)NH/3D HBHACACO and 3D-(HB)CB-CANH/3D-(HB) CBCACO experiments that include also the sidechain resonances [100].

3.2.2.3. Interleaved experiments and the UTOPIA sequences. Interleaved acquisition has been used in NMR of small molecules in liquids [26,92,101], solids NMR [102] as well as in MRI [103]. A pulse scheme combining ^{1}H-^{15}N NOESY-TROSY that is interleaved with the ^{13}C-^{13}C TOCSY sequence has been named UTOPIA (Unified Time-OPtimized Interleaved Acquisition) [104]. The second UTOPIA experiment interleaves 3D HNCA and NCO pulse schemes. The UTOPIA experiments offer a significant time saving as compared with the conventional way of recording the experiments sequentially. The experiments were performed using a single receiver and fast switching of the receiver frequency between the two interleaved experiments.

$$H\alpha_i, t_1 \xrightarrow{J_{HC}} C\alpha_i \rightarrow \boxed{\begin{array}{c} 2\tau_C,\ 2\tau_{CN} \\ \text{Polarization} \\ \text{Sharing} \end{array}} \begin{array}{l} \rightarrow N_{i,i+1}, t_2 \xrightarrow{J_{NH}} H_{i,i+1},\ t_3 \\ \\ \rightarrow C\alpha_i, t'_2 \xrightarrow{J_{C\alpha CO}} CO_i,\ t'_3 \end{array}$$

Scheme 1.

The first pulse scheme combines experiments with largely independent coherence transfer pathways. In perdeuterated proteins, such as of U-[^{2}H,^{13}C,^{15}N] labelled (fully ^{1}H back-exchanged) soluble Bcl-x_L protein (21 kDa) used for the tests, ^{1}H-decoupling is usually not necessary leaving the proton magnetization undisturbed during the ^{13}C-^{13}C TOCSY experiment of the ^{1}H-^{15}N NOESY-TROSY/^{13}C-^{13}C TOCSY sequence. The signal intensities in the interleaved experiments were essentially (95%) unperturbed when compared with the corresponding spectra recorded using the conventional approach.

In the interleaved HNCA/CON experiment the disturbance of the ^{13}CO spins of the CON experiment by the HNCA pulse sequence is minimized by moving the joint recycle delay in between the two experiments and using suitable ^{1}H decoupling pulses. No difference in the information content as compared to the conventional experiments was observed.

3.2.3. Multiple receiver experiments in metabolomics

Analysis of NMR spectra in metabolomics research is typically complicated by strong overlap of resonances. Therefore resonance assignment requires use of two-dimensional techniques, such as 2D TOCSY, 2D ^{13}C HSQC and 2D or 3D HSQC-TOCSY or TOCSY-HSQC. Such experiments can be very time consuming. Atreya, *et al.* have proposed a dual receiver experiment combining the dual receive 2D TOCSY/HETCOR [18] with reduced dimensionality (TILT [105]) 3D HSQC-TOCSY experiment for use in metabolomics research [106]. The 2D TOCSY and a tilted plane of the 3D HSQC-TCOSY spectra are recorded in a time-shared fashion. Thus the 3D HSQC-TOCSY spectral information can be recovered from the two orthogonal (H-H TOCSY and H-C HETCOR) planes and two tilted HSQC-TOCSY planes. The magnetization transfer pathways for this experiment are summarized below (Scheme 2):

Combined with non-uniform sampling [9–11,17] the technique reduces the acquisition time by more than an order of magnitude as compared to the conventional techniques (sensitivity permitting). The spectra of a mixture containing 21 metabolites in the 1 mM concentration range have been recorded on an 800 MHz NMR system equipped with a cryogenic probe.

3.3. Spatial encoding techniques

3.3.1. Ultra-fast multi-FID NMR techniques – PUFSY and HSQC/HMBC

The principles of spatial encoding techniques have been recently reviewed by Dumez [107] and will not be discussed in detail here. The ultra-fast (UF) NMR spectroscopy is based on spatiotemporal encoding principles and has a unique capability to deliver multi-dimensional NMR spectra in a single scan (sensitivity permitting) [2,3]. One of the possible ways to combine this unique methodology with parallel acquisition technique is shown in Fig. 8a (PUFSY – Parallel Ultra-Fast SpectroscopY). The first hard ^{1}H 90° pulse is followed by two adiabatic CA-WURST pulses in the presence of bipolar gradient pulses $\pm G_e$ that form the spatiotemporal encoding element. The N-loops of data acquisition in the presence of bipolar decoding gradient, $\pm G_a$ generate the required 2D data matrix. The two coherence selection gradients flanking the *X* read pulse prepare the required ^{1}H and X coherence components for the following decoding and detection. Note that the ^{1}H nuclei are affected by the sum of the two gradients while the X nuclei only experience the gradient that follows the X read

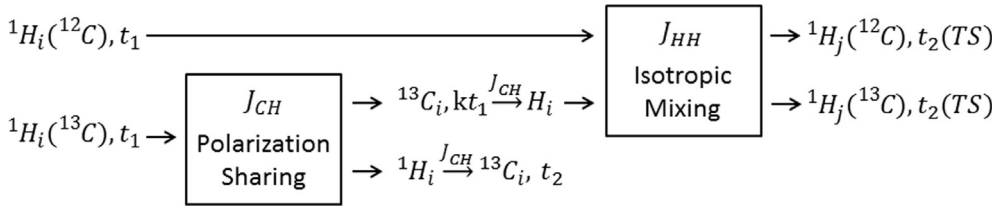

Scheme 2.

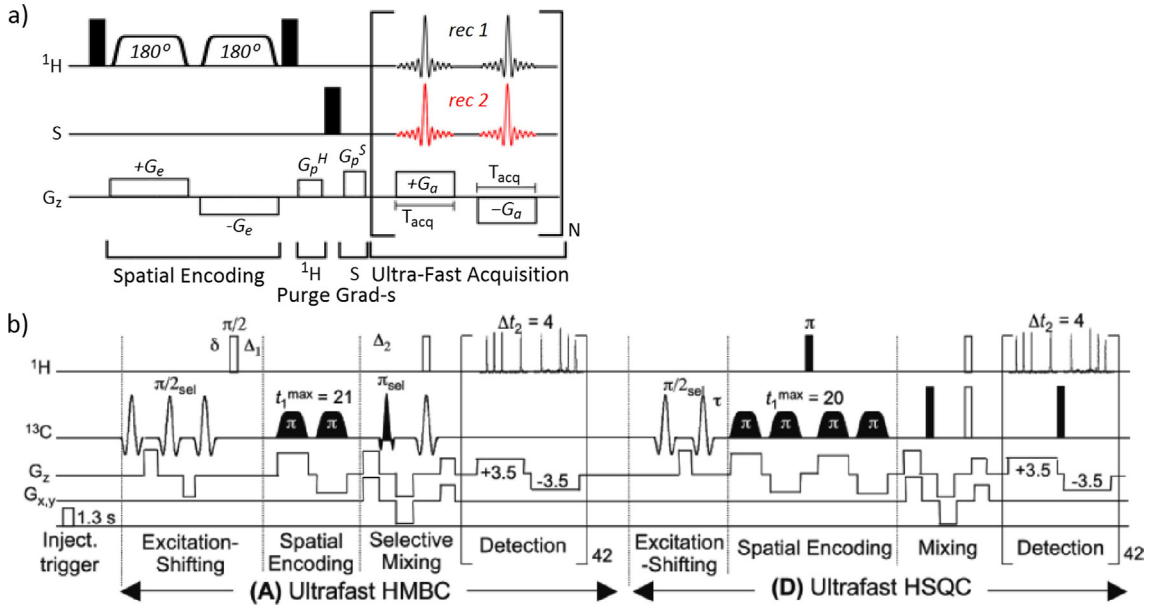

Fig. 8. (a) The PUFSY-COSY pulse sequence for simultaneous acquisition of H-H COSY and H-X COSY in a single scan (S is spin ½ nuclei); the filled rectangles are square π/2 pulses, the rounded rectangles are adiabatic (WURST) π pulses. Reproduced from [108] with permission. (b) The pulse scheme for interleaved ultra-fast 2D ^{13}C-^{1}H HMBC/HSQC experiment. The hollow rectangles are square π/2 pulses, the rounded filled rectangles are adiabatic π pulses. Reproduced from [109] with permission.

pulse providing the desired γ-based coherence selection. Just like in the conventional PANSY-COSY experiments the F1 (^{1}H) dimension is shared in the PUFSY-COSY experiments [108].

The PUFSY technique provides new opportunities for high-throughput analyses, chemical kinetics, and fast experiments on metastable hyperpolarized solutions. The experiment has been demonstrated for S = ^{19}F and ^{31}P.

The interleaved UF 2D ^{13}C-^{1}H HSQC/HMBC pulse scheme has been designed for applications in hyperpolarized samples [109]. One of the limitations of single-scan UF 2D NMR experiments is their inability to cover wide spectral ranges that require strong acquisition gradients. This is of a particular concern in UF ^{13}C NMR experiments. A new spatial/spectral encoding technique proposed by Giraudeau, *et al.* overcomes this problem by "shifting" ^{13}C resonances to arbitrary positions in UF NMR spectra. In this way multiple heteronuclear correlations arising from different ^{13}C spectral regions can be recorded. The technique enabled consecutive acquisition of UF ^{13}C-^{1}H HMBC and HSQC spectra of *ca.* 1 mM mixtures of natural products, characterized with high resolution sites spread over ~70 ppm spectral bandwidths [109]. The pulse sequence is shown in Fig. 8b.

The UF 2D ^{13}C-^{1}H HMBC module starts with a series of selective excitation pulses on the non-protonated ^{13}C sites, followed by magnetic field gradients imposing site-specific spatial encoding. If suitably chosen these gradients will shift the indirect-domain ^{13}C resonances to arbitrary positions within the ultrafast 2D spectrum reducing the final spectral window and minimizing the required strength of the acquisition gradients. This is followed by a constant-time spatial encoding, additional evolution delays, pulses and coherence selective gradients designed to filter out the sought C-H correlations.

Note that except for the ^{13}C sites that were selected, all remaining ^{13}C sites retain their initial hyperpolarized state. This allows additional experiments exploiting the hyperpolarized state of the low-γ nuclei to be recorded immediately after the UF 2D HMBC spectrum is acquired, such as UF 2D HSQC experiment that provides information about directly bonded ^{13}C-^{1}H spin pairs without the need to repolarize the sample. The UF 2D HSQC based on similar spectral/spatial encoding schemes is started immediately after the HMBC module. The UF 2D HMBC/HSQC experiments enabled characterization of ^{13}C bandwidths in excess of 70 ppm with high resolution in both the indirect and direct domains.

3.3.2. The PALSY method

The PALSY technique (PArallel Localized SpectroscopY) [110] is based on slice selective excitation in a regular (5 mm) NMR sample tube and allows recording several 2D spectra in a single experiment. The sample is virtually divided into a discrete number of non-overlapping slices that relax independently during consecutive scans of the experiment. 2D COSY, 2D DQF-COSY and 2D TQF-COSY spectra have been recorded simultaneously in 3 min with 128 increments in the t_1 dimension.

3.3.3. NMR of multiple samples using spatial encoding

Up to 19 capillary samples have been placed in a single NMR coil and their spectra separated using the spectral localization

technique [111]. Note that more than M gradient increments are required to obtain M clean spectra with these methods making this intrinsically a slow technique. Furthermore, the sensitivity is low due to the low effective filling factor for each individual sample.

The SUSHY technique (Spectral Unravelling by Space-selective Hadamard spectroscopY) proposed by Murali, *et al.* [112] allows recording NMR spectra from up to 4 samples simultaneously using the regular NMR probes and standard configuration of NMR hardware. Up to four sample tubes are loaded in a modified spinner turbine and a standard 5 mm liquids NMR probe equipped with triple axis gradients. The individual spectrum from each sample is extracted by adding and subtracting data that are recorded simultaneously from all the samples combining the principles of spatially resolved spectroscopy and Hadamard encoding [13]. This technique has a potential to reduce the total experimental time by up to a factor of four in a 4-tube mode. Note, however, that in the 4-sample setup a minimum of four scans per time increment is required for the Hadamard encoding/decoding to work. The approach is akin to the *TS* technique [27].

4. Multiple FID detection in solid-state NMR

Like solution-state NMR, a major part of most of the solid-state NMR experiments routinely used consists of the T_1-recovery delay. Under these conditions, the prerequisites for acquiring multiple experiments remain exactly the same as those described for solution state: (a) the ability to generate multiple polarization pathways, (b) co-evolve or evolve them independently and (c) store one or more of these pathways and recover the polarization from these at a later stage. Several aspects of solid-state NMR make all of these conditions particularly straightforward to achieve. The following sections discuss these in depth.

4.1. Generating, storing and detecting multiple coherence pathways: Basic principles

4.1.1. Generating multiple coherence pathways

The initial step in a majority of biomolecular solid-state NMR experiments is often cross-polarization from ^{1}H to a low-gamma nucleus such as ^{13}C or ^{15}N. Cross-polarization is a bulk phenomenon, i.e. we expect transfer from a proton bath to each nucleus. However, the proton-baths connected to ^{15}N and ^{13}C can be considered to be independent sources of polarization for the two distinct nuclei, and one can simultaneously transfer polarization to ^{15}N and ^{13}C without losing a majority of the signal. To the best of our knowledge, this was first used in experiments on biomolecules by Ramachandran and co-workers [113], who used it to transfer polarization simultaneously to ^{13}C and ^{15}N in labelled RNA samples. Reif and co-workers used this method to transfer polarization to methyl-^{13}C and amide-^{15}N nuclei in proteins [114]. Veglia and co-workers showed that this was indeed a general scheme to transfer polarization to heteronuclei connected to different protons [76]. They systematically analysed the build-up of polarization on the two nuclei when they are cross-polarized from ^{1}H independently and simultaneously and showed that the build-up rates are indeed similar in both the cases. These experiments show that under conditions optimized for ^{13}C cross-polarization, ~80% of the sensitivity can be obtained by simultaneously cross-polarizing to the ^{15}N nuclei. This strategy also was later exploited in experiments by Nielsen, *et al.* [115], Lamley, *et al.* [116] and Takeda, *et al.* [117] to acquire multiple ^{13}C and ^{15}N experiments simultaneously on protein samples. Experiments from Das and Opella [28] and our lab (unpublished data) show that this strategy gives similar results with fast MAS [118] and double-quantum cross-polarization transfers from ^{1}H to ^{13}C and ^{15}N in proteins. In general, it seems possible that given samples with two different nuclei connected to protons, it should be possible to simultaneously cross-polarize these nuclei. A related method is the simultaneous cross-polarisation from ^{1}H and ^{2}H to ^{13}C in deuterated proteins [119] that improves sensitivity in these samples. This method can in principle be adapted to transfer to multiple nuclei (^{15}N and ^{13}C), but experimental demonstration of this is yet lacking.

4.1.2. Storing and detecting multiple coherences

One of the reasons for the success of sequential MFD experiments in solid-state NMR is the long T_1 relaxation of ^{15}N in solids [120]. After ^{13}C and ^{15}N nuclei are cross-polarized, the ^{15}N magnetization can hence be stored as longitudinal polarization and the experiment is continued with the ^{13}C-edited part in an unhindered manner. At a later stage, the stored polarization can be recalled and used in a second experiment before the recycle delay. Unlike in solutions, where the T_1 time for ^{15}N can be of the order of a few seconds, T_1 time in solids is of the order of minutes, and virtually no loss of polarization occurs. Moreover, spin diffusion is inefficient between ^{15}N nuclei in static and rotating solids, requiring > 2 sec mixing time [121–123]. Thus, magnetization can be stored not only at the initial stage, but at almost any step of the pulse sequence without significant build-up of cross-peaks to nearby ^{15}N nuclei. With the above two strategies Veglia and co-workers showed that the two most commonly used experiments in solid-state NMR, DARR and NCa can be combined into a single experiment (Fig. 9A) [76]. Since in proteins amide ^{15}N have a much smaller chemical-shift spread than ^{13}C nuclei, and the relaxation times for the two nuclei can be quite different, the ability to have complete control over these parameters (spectra width and evolution times) is of critical importance. The main restriction in doing the experiment as described above is that the total number of indirect points in the ^{13}C and ^{15}N dimensions has to be identical. Although this might seem restrictive *prima facie*, the ^{15}N-edited experiments can be reset to the first dwell time at any increment. Thus, multiple ^{15}N experiments (with a smaller number of increments per data point and a smaller spectral width, together giving the desired t_1-evolution time) can be acquired and added up at the end. The power of this experiment is more apparent in cases where sufficient sensitivity can be obtained for the ^{15}N experiments with the same number of scans as the ^{13}C experiment. In these cases, the ^{15}N-edited experiment can itself be switched on after a desired t_1-evolution time is reached. Here, multiple experiments such as NCα, NC', N(Cα)Cx and N(C')Cx can be recorded, each with a fraction of the number of increments of the ^{13}C-edited experiment, but with a smaller spectral width, resulting in the desired evolution time for ^{15}N. In a similar manner, one can acquire ^{13}C-^{13}C Double-Quantum/Single-Quantum (DQSQ) correlation spectrum alongside the ^{15}N-edited experiments as well.

If the ^{15}N and ^{13}C edited experiments are to be kept completely independent as described in the above example, there are relatively few experiments of routine use that can be extended to the third dimension. However, one example is CCC, where the carbon edited experiment can be kept completely independent and a NCaCx or any other ^{15}N-edited experiment can be acquired after the CCC experiment is done. A bigger set of options arises when we allow for ^{1}H detection, either using windowed detection and homonuclear decoupling [116] or fast MAS frequencies [28]. The standard CH and NH spectra can be acquired using a simple extension of this strategy, as shown in Fig. 9B. Similarly, the 3D-CHH and 3D-NHH spectra, which remain two of the most useful experiments for obtaining restraints using fast-MAS [124], can be acquired as a simple extension of this strategy [125]. Perhaps the most useful way in which this can be extended to the third dimension is by acquiring a 2D experiment that requires a significantly

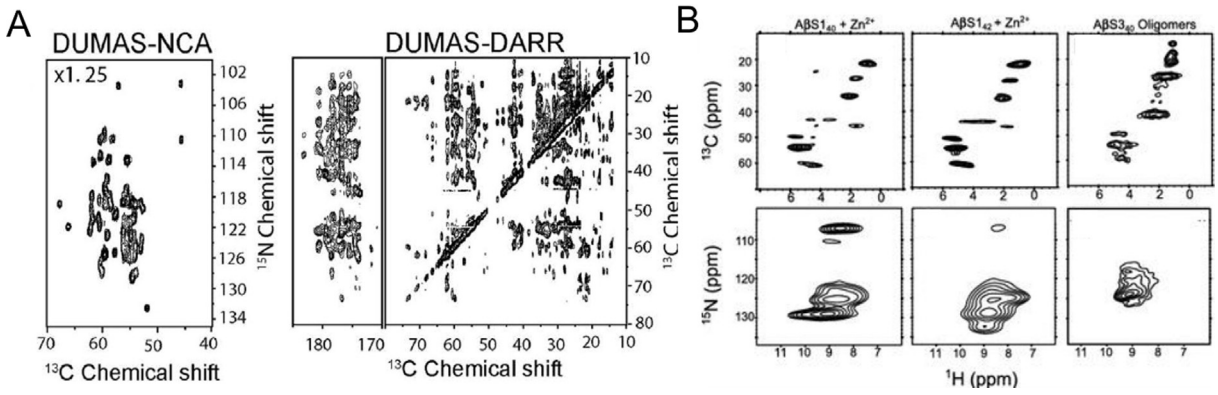

Fig. 9. (A) Sequentially detected NCa and DARR spectra using ^{13}C detection on a sample of ubiquitin and (B) sequentially detected CH and NH spectra on different samples of amyloid-beta using ^{1}H detection. Reproduced from [76] and [125] with permission.

larger number of increments (for example, a DARR or DQSQ-correlation on uniformly ^{13}C labelled sample) alongside a 3D-NCαCx or 3D-NC'Cx experiment [125]. In the specific case of the DARR experiments, the shorter 2D experiment can also be repeated with different mixing times while the 3D experiments are running.

4.2. Multiplex phase cycling to combine experiments

In order to fully exploit the multiple polarization pathways generated, standard experiments that involve the transfer of magnetization from ^{13}C to ^{15}N and *vice versa* have to be brought under the purview of this strategy. This can be done in a straightforward way by using a slightly modified version of multiplex phase cycling [126]. This is best described using an example of a combination of two standard 3D experiments: NCCx and CaNC', shown in Fig. 10A. Cross-polarization serves to effectively exchange and equilibrate magnetization on spins using dipolar or scalar couplings and, thus, the central SPECIFIC-CP block serves to effectively *exchange* the initial magnetization of ^{15}N and ^{13}C. In order to recover both these experiments, we can use the fact that they have common pulse blocks, and that the receiver phase can be independently set for each of the acquisitions, as shown in the figure caption. With this strategy, one can design a number of combinations from among the most widely used pulse sequences for assignment. Gopinath and Veglia [127] have used this strategy to extend the multiple detection scheme to 3D and 4D experiments. The combination of NCaCx and CaNCo is shown in Fig. 10B. A similar strategy has also been earlier utilized by Takegoshi and co-workers to acquire a COSY and a DARR spectrum simultaneously [56].

Looking at this strategy from a wider perspective, we see analogies with well established sensitivity enhancement schemes in solution NMR [128] and oriented NMR [129,130], where a source of polarization that would otherwise be discarded is recovered. The difference is that in this case, the additional source of polarization is not a part of the original experiment, but is generated by the initial simultaneous cross-polarization.

4.3. Residual polarization pathways

Solid-state NMR pulse sequences are often inefficient. For example, the maximum theoretical efficiency of a cross-polarization sequence is ~73%. This means than under ideal conditions, close to 30% of the initial polarization remains un-utilised in an experiment involving a single cross-polarization step. One of the places where this inefficiency leads to large losses in sensitivity is the transfer of polarization from ^{13}C to ^{15}N and vice versa. The theoretical efficiency is far from being achieved in many of the applications, and experimental transfer efficiency close to 40–50% for transfers is quite common. CP transfer steps that involve an unmodulated RF field on ^{15}N will result in the magnetization being spin-locked along the direction of the B_1 field at the end of the CP-block. Traaseth and co-workers [78] showed that this 'residual' polarization can be stored as longitudinal polarization with a simple $\pi/2$ pulse after the CP step, which can then be recovered at a later stage for additional experiments (Fig. 11A).

Veglia and co-workers generalised this scheme to recover residual polarizations from both ^{13}C and ^{15}N in a single experiment using multiplex phase cycling [131] and showed that one can use this to rapidly assign resonances in challenging samples in the solid state [132]. The power of this approach can be seen from the fact that each CP transfer step among ^{13}C and ^{15}N generates four pathways that can be recovered, instead of a single experiment that is collected using traditional phase cycling (Fig. 11B). These experiments are additive, i.e. if the experiment of interest has two CP steps, a total of $4 \times 2 = 8$ experiments can be collected. Not all of the experiments collected this way are meaningful, for example they can have duplication of a frequency label in two axes. Repeated cross-polarization transfers as described above will have increasingly lower levels of polarization being recovered; four consecutive ^{15}N to ^{13}C transfers were shown to result in 100%, 30%, 10% and 3% of the net polarization being recovered at each step [133]. Such an experimental design is comparable to repetitive CP but has an advantage in multidimensional experiments as none of the indirect dimensions need to be encoded again. This strategy is useful not only in MAS, but also in oriented solid-state NMR to obtain proton-drive spin diffusion-edited PISEMA (Polarization Inversion Spin Exchange at Magic Angle) spectrum along-side a control PISEMA spectrum [134]. The power of residual polarisations in biomolecular solid-state NMR goes much beyond sensitivity gains, impressive as they may be. Traaseth and co-workers showed that with appropriate labelling and un-labelling schemes, residual polarization can be used as a handy tool to simplify crowded spectra [135]. For example, in absence of ^{13}C labelled carbonyl carbons, a ^{15}N to ^{13}C' transfer will leave essentially 100% of the initial polarization as 'residual'. A subsequent ^{15}N to ^{13}C transfer will then show 100% intensity (as compared to a simple ^{15}N to ^{13}C transfer), rather than the 30% as described above. For example, if a proteins sample on a uniformly ^{13}C and ^{15}N background is made in such a way that all isoleucines remain unlabelled (by simply adding unlabelled isoleucine before induction), an ^{15}N-^{13}C spectrum following a ^{15}N-^{13}C' transfer will result primarily in resonances that are immediately after isoleucine in the primary sequence. This considerably simplifies assignments which would have been otherwise impossible to obtain (Fig. 12).

The combination of a) simultaneous cross-polarization to multiple nuclei, b) multiplex phase cycling and c) residual polarization

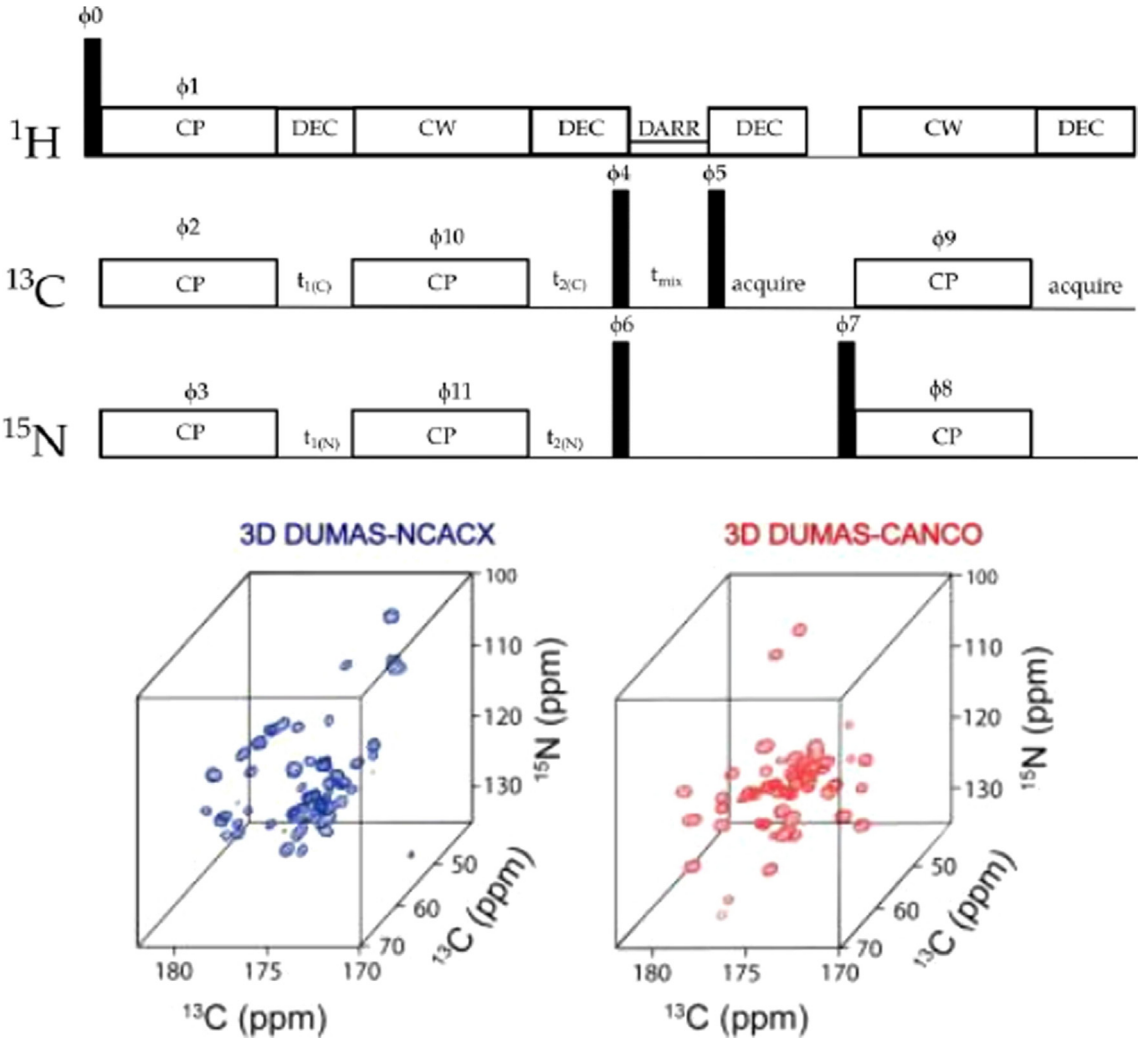

Fig. 10. (A) Pulse sequence for the sequential acquisition of NCαCx and CαNCO experiments. The phase of the signal for the first acquisition (NCαCx) is given by: Φ(common) + Φ3 + Φ4 - Φ5, whereas that for the second acquisition is given by Φ(common) + Φ2 + Φ6 - Φ7 + Φ8 + Φ9. Note that one needs to avoid all other pathways by phase cycling Φ9 and Φ10 blocks. (B) 3D NCαCx and 3D-CαNCO spectra acquired using a pulse sequence similar to that in A. Reproduced from [127] with permission.

after transfers can all be combined along with ^{1}H and ^{13}C detection to give virtually unlimited combination of experiments that can be done in solid-state NMR. Excellent examples of this combination are given by the experiments described by the group of Veglia [131,132]. Here as many as four 2D experiments or three 3D experiments could be combined in a single experiment resulting in time savings on the order of 70%. When combined with ^{1}H detection, the number of combinations increases even further and as many as four experiments can be recovered using a single FID acquisition [125]. With multiple FIDs, this number only goes up, and Veglia and co-workers [133] were able to recover 8 experiments from 4 sequentially acquired FIDs. For ^{13}C detection with protein samples, these experiments are best done with Low-E/E-free probes that can tolerate the increased duty cycle with minimal increase in sample heating. ^{1}H detected experiments at fast MAS frequencies stand to gain the most from these strategies, as these experiments can be done using low RF amplitudes and will not suffer from the drawbacks related to increased duty cycles. With these strategies in hand, virtually any ^{13}C-edited and ^{15}N-edited experiments in biomolecular solid-state NMR can be effectively combined and acquired in sequentially detected manner, or can be deconvoluted using multiplex phase cycling.

5. Conclusions

Experiments with direct multiple FID detection provide more information in a single measurement as compared to the conventional way of recording the NMR spectra in consecutive fashion. Furthermore, such experiments lead to significant time savings, offer better sensitivity per unit time and often provide the same information as similar conventional experiments of higher dimensionality.

There are two main categories of multi-FID detection schemes – experiments with homonuclear detection and multinuclear detected experiments enabled by the advent of multiple receiver technologies in NMR. The basic data acquisition techniques in each of these two categories are loosely classified into parallel acquisition, sequential acquisition and interleaved experiments. More sophisticated MFD schemes involve mixed data acquisition modes.

There are several approaches in designing the MFD experiments. One of the most popular methods is based on the PEP principles. Two or more coherence pathways are preserved and utilized to record different types of multi-dimensional NMR spectra. Alternatively the residual magnetization left after recording the FIDs of low gamma nuclei (the 'afterglow') is transferred to sensitive

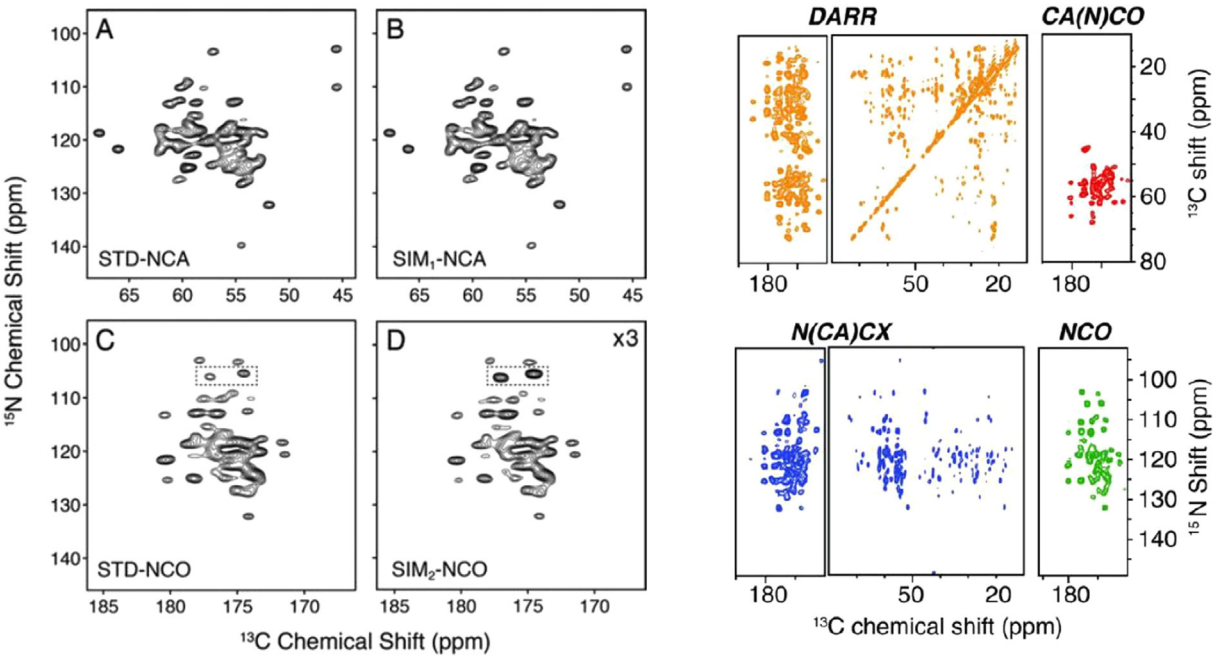

Fig. 11. A comparison of independently acquired (A, C) and sequentially acquired (B, D) NCα and NCO spectra on microcrystalline ubiquitin. (F) Sequentially acquired DARR, Cα(N)CO, N(Cα)Cx and NCO spectra using the residual polarization pathways and multiplex phase cycling. Reproduced from [131] and [78] with permission.

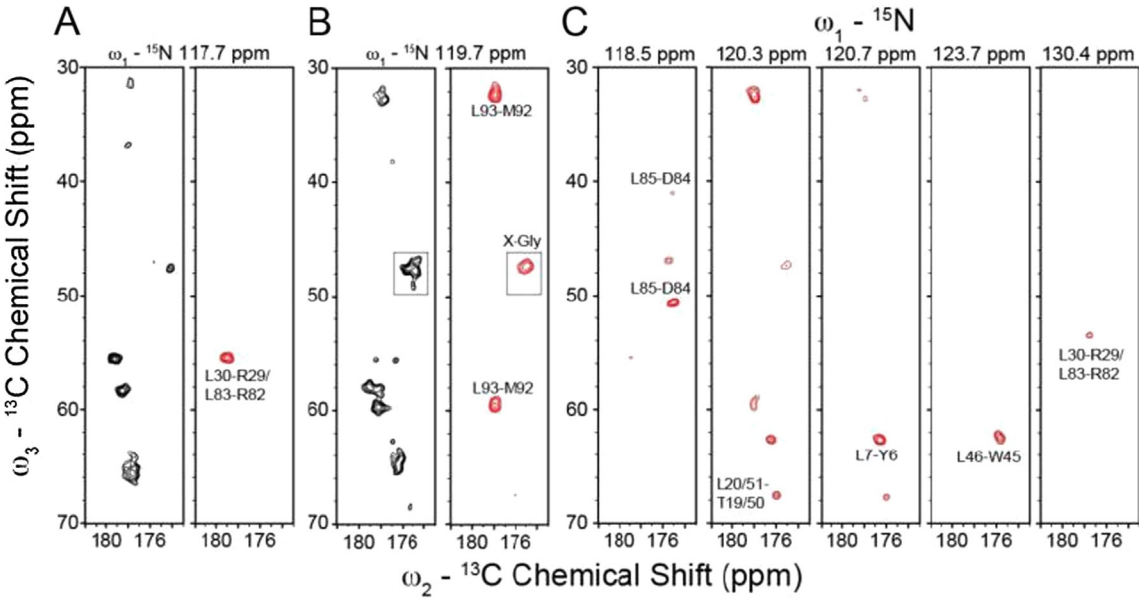

Fig. 12. NCoCx spectra acquired on uniformly ^{13}C and ^{15}N labelled EmrE (black) and ^{15}N-Leu-unlabelled EmrE (all amino acids except Leu is ^{13}C and ^{15}N labelled, while all leucines are ^{15}N labelled). In the residual polarization spectra, only the resonance that are just after Leucine are seen and are directly assigned based on the primary sequence. (A) and (B) show a direct comparison between a uniformly labelled EmrE and ^{15}N-Leu-unlabelled EmrE. (C) shows several strip plots from the ^{15}N-Leu-unlabelled EmrE corresponding to the residues preceding all leucines. Reproduced from [131] and [78] with permission.

nuclei, typically ^{1}H for detection. Isotope filtering techniques are employed in small molecule NMR for separating various isotopomers that exist at the natural abundance of isotopes in small organic molecules. The NOAH and PANACEA pulse schemes combine several such techniques allowing structure elucidation of small molecules from a single measurement. Similar combinations of higher dimensionality experiments in biomolecular NMR provide resonance assignments in proteins from a single measurement.

One of the challenges in the MFD experiments involving direct detection of low gamma nuclei is the large differences in signal sensitivities in ^{1}H and X-nuclei detected spectra. The latest generation cryogenic probes largely alleviate this problem. In parallel sequential acquisition pulse schemes the problem can be addressed by balancing the coherence flows in favour of less sensitive nuclei. In interleaved experiments pulse schemes producing spectra of comparable signal-to-noise ratio are paired. In general, the multinuclear MFD experiments are useful in situations when

strong samples are available and the X-nuclei detected spectra are of prime interest while the ^{1}H detected spectra provide complementary information concurrently. This point is sometimes overlooked [74].

In solids the combination of (a) simultaneous cross-polarization to multiple nuclei, (b) multiplex phase cycling and (c) residual polarization after transfers can all be combined along with ^{1}H and ^{13}C detection to give virtually unlimited combination of MFD experiments. Such approaches will greatly enable assignments and subsequent structure and/or dynamics elucidation of molecules in a faster way being particularly helpful for samples with limited stability. Analysis of challenging systems, such as membrane proteins, will benefit from MFD schemes.

Declaration of Competing Interest

None.

References

[1] L. Rouger, B. Gouilleux, P. Giraudeau, Fast n-dimensional data acquisition methods, Encyclopedia of Spectroscopy and Spectrometry (Third Edition) 588–596 (2017).
[2] L. Frydman, T. Scherf, A. Lupulescu, The acquisition of multidimensional NMR spectra within a single scan, Proc. Natl. Acad. Sci. U.S.A. 99 (2002) 15858–15862.
[3] A. Tal, L. Frydman, Single-scan multidimensional magnetic resonance, Prog. NMR Spectrosc. 57 (2010) 241–292.
[4] P. Schanda, B. Brutscher, Very fast two-dimensional NMR spectroscopy for real-time investigation of dynamic events in proteins on the time scale of seconds, J. Am. Chem. Soc. 127 (2005) 8014–8015.
[5] P. Schanda, Ē. Kupče, B. Brutscher, SOFAST-HMQC experiments for recording two-dimensional heteronuclear correlation spectra of proteins within a few seconds, J. Biomol. NMR 33 (2005) 199–211.
[6] P. Schanda, H. Van Melckebeke, B. Brutscher, Speeding up three-dimensional protein NMR experiments to a few minutes, J. Am. Chem. Soc. 128 (2006) 9042–9043.
[7] Ē. Kupče, R. Freeman, Fast multidimensional NMR by polarization sharing, Magn. Reson. Chem. 45 (2007) 2–4.
[8] D. Schulze-Sünninghausen, J. Becker, M.R.M. Koos, Burkhard Luy, Improvements, extensions, and practical aspects of rapid ASAP-HSQC and ALSOFAST-HSQC pulse sequences for studying small molecules at natural abundance, J. Magn. Reson. 281 (2017) 151–161.
[9] J.C.J. Barna, E.D. Laue, M.R. Mayger, J. Skilling, S.J.P. Worrall, Exponential sampling, an alternative method for sampling in two-dimensional NMR experiments, J. Magn. Reson. 73 (1987) 69–77.
[10] M. Mobli, J.C. Hoch, Nonuniform sampling and non-Fourier signal processing methods in multidimensional NMR, Prog. NMR Spectrosc. 83 (2014) 21–41.
[11] K. Kazimierczuk, J. Stanek, A. Zawadzka-Kazimierczuk, W. Koźmiński, Random sampling in multidimensional NMR spectroscopy, Prog. NMR Spectrosc. 57 (2010) 420–434.
[12] Ē. Kupče, R. Freeman, Two-dimensional hadamard spectroscopy, J. Magn. Reson. 162 (2003) 300–310.
[13] Ē. Kupče, T. Nishida, R. Freeman, Hadamard NMR spectroscopy, Prog. NMR Spectrosc. 42 (2003) 95–122.
[14] Ē. Kupče, R. Freeman, Fast multidimensional NMR: radial sampling of evolution space, J. Magn. Reson. 173 (2005) 317–321.
[15] B.E. Coggins, R.A. Venters, P. Zhou, Radial sampling for Fast NMR: Concepts and practices over three decades, Prog. NMR Spectrosc. 57 (2010) 381–419.
[16] Ē. Kupče, R. Freeman, SPEED: single-point evaluation of the evolution dimension, Magn. Reson. Chem. 45 (2007) 711–713.
[17] A.L. Hansen, R. Brüschweiler, Absolute minimal sampling in high-dimensional NMR spectroscopy, Angew. Chem. Int. Ed. 55 (2016) 14169–14172.
[18] Ē. Kupče, R. Freeman, B.K. John, Parallel acquisition of two-dimensional NMR spectra of several nuclear species, J. Am. Chem. Soc. 128 (2006) 9606–9607.
[19] Ē. Kupče, R. Freeman, NMR spectroscopy using several parallel receivers, R. Freeman and Ē. Kupče, in: A.J. Williams, G.E. Martin, D. Rovnyak, (Eds.), Modern NMR Approaches To The Structure Elucidation of Natural Products, vol. 1, Ch. 7, pp. 117-145, Royal Soc. Chem., 2016.
[20] Ē. Kupče, R. Freeman, Hyperdimensional NMR spectroscopy, J. Am. Chem. Soc. 128 (2006) 6020–6021.
[21] Ē. Kupče, R. Freeman, Hyperdimensional NMR spectroscopy, Prog. NMR Spectrosc. 52 (2008) 22–30.
[22] V.A. Jaravine, A.V. Zhuravleva, P. Permi, I. Ibraghimov, V.Yu. Orekhov, Hyperdimensional NMR spectroscopy with nonlinear sampling, J. Am. Chem. Soc. 130 (2008) 3927–3936.
[23] Yu. Pustovalova, M. Mayzel, V.Yu. Orekhov, "XLSY: Extra-Large NMR spectroscopy, Angew. Chem. Int. Ed. 57 (2018) 14043–14045.
[24] C.A.G. Haasnoot, F.J.M. van de Ven, C.W. Hilbers, COCONOSY. Combination of 2D correlated and 2D nuclear Overhauser enhancement spectroscopy in a single experiment, J. Magn. Reson. 56 (1984) 343–349.
[25] Ē. Kupče, T.D.W. Claridge, NOAH: NMR supersequences for small molecule analysis and structure elucidation, Angew. Chem. Int. Ed. 56 (2017) 11779–11783.
[26] H. Kovacs, Ē. Kupče, Parallel NMR spectroscopy with simultaneous detection of ^{1}H and ^{19}F nuclei, Magn. Reson. Chem. 54 (2016) 544–560.
[27] T. Parella, P. Nolis, Time-shared NMR experiments, Concepts Magn. Reson. 36A (2010) 1–23.
[28] B.B. Das, S.J. Opella, Multiple acquisition/multiple observation separated local field/chemical shift correlation solid-state magic angle spinning NMR spectroscopy, J. Magn. Reson. 245 (2014) 98–104.
[29] K.R. Thulborn, N.F. Soffe, G.K. Radda, Simultaneous in vivo measurement of oxygen utilization and high-energy phosphate metabolism in rabbit skeletal muscle by multinuclear ^{1}H and ^{31}P NMR, J. Magn. Reson. 45 (1981) 362–366.
[30] M. Hutchinson, U. Raff, Fast MRI data acquisition using multiple detectors, Magn. Reson. Med. 6 (1988) 87–91.
[31] J.W. Carlson, An algorithm for NMR imaging reconstruction based on multiple RF receiver coils, J. Magn. Reson. 74 (1987) 376–380.
[32] D. Kwiat, S. Einav, G. Navon, A decoupled coil detector array for fast image acquisition in magnetic resonance imaging, Med. Phys. 18 (1991) 251–265.
[33] U. Katscher, P. Börnert, Parallel Magnetic Resonance Imaging, Neurotherapeutics 4 (2007) 499–510.
[34] A. Deshmane, V. Gulani, M.A. Griswold, N. Seiberlich, Parallel MR imaging, J. Magn. Reson. Imaging 36 (2012) 55–72.
[35] S. Chakraborty, S. Paul, R.V. Hosur, Simultaneous acquisition of ^{13}Cα-^{15}N and ^{1}H–^{15}N-^{15}N sequential correlations in proteins: application of dual receivers in 3D HNN, J. Biomol. NMR 52 (2012) 5–10.
[36] A.G. Webb, Microcoil nuclear magnetic resonance spectroscopy, J. Pharm. Biomed. Anal. 38 (2005) 892–903.
[37] A.G. Webb, J.V. Sweedler, D. Raftery, Parallel NMR Detection, in: K. Albert, (Ed.), On-Line LC-NMR and Related Techniques, John Wiley & Sons, Ltd, Ch. 8.2, 2002, pp. 259–279.
[38] O. Gökay, K. Albert, From single to multiple microcoil flow probe NMR and related capillary techniques: a review, Anal. Bioanal. Chem. 402 (2012) 647–669.
[39] B.T. Farmer II, Simultaneous [^{13}C,^{15}N]-HMQC, a pseudo-triple-resonance experiment, J. Magn. Reson. 93 (1991) 635–641.
[40] B.T. Farmer, L. Mueller, Simultaneous acquisition of [^{13}C, ^{15}N]- and [^{15}N, ^{15}N]-separated 4D gradient-enhanced NOESY spectra in proteins, J. Biomol. NMR 4 (1994) 673–687.
[41] S.M. Pascal, D.R. Muhandiram, T. Yamazaki, J.D. Forman-Kay, L.E. Kay, Simultaneous acquisition of ^{15}N- and ^{13}C-edited NOE spectra of proteins dissolved in H_2O, J. Magn. Reson. 103B (1994) 197–201.
[42] F. Lohr, A. Laguerre, C. Bock, S. Reckel, P.J. Connolly, N. Abdul-Manan, F. Tumulka, R. Abele, J.M. Moore, V. Dotsch, Time-shared experiments for efficient assignment of triple-selectively labelled proteins, J. Magn. Reson. 248 (2014) 81–95.
[43] D. Yang, K. Nagayama, A sensitivity-enhanced method for measuring heteronuclear long-range coupling constants from the displacement of signals in two 1D subspectra, J. Magn. Reson. 118 (1996) 117–121.
[44] M. Ottiger, F. Delaglio, A. Bax, Measurement of J and dipolar couplings from simplified two-dimensional NMR spectra, J. Magn. Reson. 131 (1998) 373–378.
[45] G. Kontaxis, A. Bax, Multiplet component separation for measurement of methyl ^{13}C–^{1}H dipolar couplings in weakly aligned proteins, J. Biomol. NMR 20 (2001) 77–82.
[46] T. Kern, P. Schanda, B. Brutscher, Sensitivity-enhanced IPAP-SOFAST-HMQC for fast-pulsing 2D NMR with reduced radiofrequency load, J. Magn. Reson. 190 (2008) 333–338.
[47] C. Richter, H. Kovacs, J. Buck, A. Wacker, B. Fürtig, W. Bermel, H. Schwalbe, ^{13}C-direct detected NMR experiments for the sequential J-based resonance assignment of RNA oligonucleotides, J. Biomol. NMR 47 (2010) 259–269.
[48] C. Fontana, H. Kovacs, G. Widmalm, NMR structure analysis of uniformly ^{13}C-labelled carbohydrates, J. Biomol. NMR 59 (2014) 95–110.
[49] A.Z. Gurevich, I.L. Barsukov, A.S. Arseniev, V.F. Bystrov, Combined COSY-NOESY experiment, J. Magn. Reson. 56 (1984) 471–478.
[50] Ē. Kupče, T.D.W. Claridge, Molecular structure from a single NMR Supersequence, Chem. Commun. 54 (2018) 7139–7142.
[51] Ē. Kupče, R. Freeman, Binomial filters, J. Magn. Reson. 99 (1992) 644–651.
[52] A. Meissner, O.W. Sorensen, Economizing spectrometer time and broadband excitation in small-molecule heteronuclear NMR correlation spectroscopy. Broadband HMBC, Magn. Reson. Chem. 38 (2000) 981–984.
[53] R. Burger, C. Schorn, P. Bigler, HMSC: Simultaneously detected heteronuclear shift correlation through multiple and single bonds, J. Magn. Reson. 148 (2001) 88–94.
[54] W. Schoefberger, J. Schlagnitweit, N. Müller, Recent developments in heteronuclear multiple-bond correlation experiments, Ann. Rep. NMR Spectros. 72 (2011) 1–60.
[55] V.M.R. Kakita, K. Rachineni, M. Bopardikar, R.V. Hosur, NMR supersequences with real-time homonuclear broadband decoupling: sequential acquisition of protein and small molecule spectra in a single experiment, J. Magn. Reson. 297 (2018) 108–112.
[56] M. Fukuchi, K. Takegoshi, Combination of ^{13}C–^{13}C COSY and DARR (COCODARR) in solid-state NMR, Solid State NMR 34 (2008) 151–153.

[57] G. Wagner, K. Wüthrich, Sequential resonance assignments in protein ^{1}H nuclear magnetic resonance spectra: Basic pancreatic trypsin inhibitor, J. Mol. Biol. 155 (1982) 347–366.
[58] J. Cavanagh, M. Rance, A combined two-dimensional relayed NOESY/TOCSY experiment, J. Magn. Reson. 87 (1990) 408–414.
[59] P. Nolis, K. Motiram-Corral, M. Perez-Trujillo, T. Parella, Interleaved dual NMR acquisition of equivalent transfer pathways in TOCSY and HSQC experiments, ChemPhysChem 20 (2019) 356–360.
[60] P. Nolis, T. Parella, Practical aspects of the simultaneous collection of COSY and TOCSY spectra, Magn. Reson. Chem. 57 (2019) S85–S94.
[61] K. Motiram-Corral, M. Pérez-Trujillo, P. Nolis, T. Parella, Implementing one-shot multiple-FID acquisition into homonuclear and heteronuclear NMR experiments, Chem. Commun. 54 (2018) 13507–13510.
[62] P. Nolis, M. Prez-Trujillo, T. Parella, Multiple FID acquisition of complementary HMBC data, Angew. Chem. Int. Ed. Engl. 46 (2007) 7495–7497.
[63] J. Cavanagh, W.J. Fairbrother, A.G. Palmer, N.J. Skelton, Protein NMR Spectroscopy. Principles and Practice, Academic Press, 2007.
[64] Ē. Kupče, R. Freeman, Molecular structure from a single NMR experiment, J. Am. Chem. Soc. 130 (2008) 10788–10792.
[65] Ē. Kupče, R. Freeman, Molecular structure from a single NMR sequence (fast-PANACEA), J. Magn. Reson. 206 (2010) 147–153.
[66] A. Bax, R. Freeman, S.P. Kempsell, Natural abundance carbon-13-carbon-13 coupling observed via double-quantum coherence, J. Am. Chem. Soc. 102 (1980) 4849–4851.
[67] A. Bax, R. Freeman, S.P. Kempsell, Investigation of ^{13}C–^{13}C long-range couplings in natural-abundance samples, J. Magn. Reson. 41 (1980) 349–353.
[68] A. Bax, R. Freeman, T.A. Frenkiel, M.H. Levitt, Assignment of carbon-13 NMR spectra via double-quantum coherence, J. Magn. Reson. 43 (1981) 478–483.
[69] M.E. Elyashberg, A.J. Williams, G.E. Martin, Computer-assisted structure verification and elucidation tools in NMR-based structure elucidation, Prog. NMR Spectrosc. 53 (2008) 1–104.
[70] J.-M. Nuzillard, Automated interpretation of NMR spectra for small organic molecules in solution, eMagRes 3 (2014) 287–294.
[71] A.V. Buevich, M.E. Elyashberg, Synergistic combination of CASE algorithms and DFT chemical shift predictions: a powerful approach for structure elucidation, verification, and revision, J. Nat. Prod. 79 (2016) 3105–3116.
[72] M. Elyashberg, A. Williams, K. Blinov, Contemporary Computer-Assisted Approaches to Molecular Structure Elucidation, Royal Society of Chemistry, Cambridge, UK, 2011.
[73] P. Kessler, M. Godejohann, Identification of tentative marker in Corvina and Primitivo wines with CMC-se, Magn. Reson. Chem. 56 (2018) 480–492.
[74] P. Bellstedt, Y. Ihle, C. Wiedemann, A. Kirschstein, C. Herbst, M. Görlach, R. Ramachandran, "Sequential acquisition of multi-dimensional heteronuclear chemical shift correlation spectra with ^{1}H detection, Sci. Rep. 4 (2014) 4490.
[75] C. Wiedemann, P. Bellstedt, A. Kirschstein, S. Häfner, C. Herbst, M. Görlach, R. Ramachandran, Sequential protein NMR assignments in the liquid state via sequential data acquisition, J. Magn. Reson. 239 (2014) 23–28.
[76] T. Gopinath, G. Veglia, Dual acquisition magic angle spinning solid-state NMR-spectroscopy: Simultaneous acquisition of multidimensional spectra of biomacromolecules, Angew. Chem. Int. Ed. 51 (2012) 2731–2735.
[77] P. Bellstedt, C. Herbst, S. Hafner, J. Leppert, M. Gorlach, R. Ramachandran, Solid state NMR of proteins at high MAS frequencies: symmetry-based mixing and simultaneous acquisition of chemical shift correlation spectra, J. Biomol. NMR 54 (2012) 325–335.
[78] J.R. Banigan, N.J. Traaseth, Utilizing afterglow magnetization from cross-polarization magic-angle-spinning solid-state NMR spectroscopy to obtain simultaneous heteronuclear multidimensional spectra, J. Phys. Chem. B 116 (24) (2012) 7138–7144.
[79] Ē. Kupče, R. Freeman, Parallel receivers and sparse sampling in multidimensional NMR, J. Magn. Reson. 213 (2011) 1–13.
[80] Ē. Kupče, NMR with Multiple Receivers, in: H. Heise, S. Matthews (Eds.), Modern NMR Methodology. Top. Curr. Chem., Springer, Berlin, Heidelberg, 2011, pp. 71–96.
[81] Ē. Kupče, NMR with multiple receivers, eMagRes 4 (2015) 721–732.
[82] J.N. Robinson, A. Coy, R. Dykstra, C.D. Eccles, M.W. Hunter, P.T. Callaghan, Two-dimensional NMR spectroscopy in Earth's magnetic field, J. Magn. Reson. 182 (2006) 343–347.
[83] Ē. Kupče, L.E. Kay, Parallel acquisition of multi-dimensional spectra in protein NMR, J. Biomol. NMR 54 (2012) 1–7.
[84] P. Gierth, A. Codina, F. Schumann, H. Kovacs, Ē. Kupče, Fast experiments for structure elucidation of small molecules: Hadamard NMR with multiple receivers, Magn. Reson. Chem. 53 (2015) 940–944.
[85] D. Jeannerat, High resolution in heteronuclear ^{1}H–^{13}C NMR experiments by optimizing spectral aliasing with one-dimensional carbon data, Magn. Reson. Chem. 41 (2003) 3–17.
[86] Ē. Kupče, R. Freeman, High-resolution NMR correlation experiments in a single measurement (HR-PANACEA), Magn. Reson. Chem. 48 (2010) 333–336.
[87] Ē. Kupče, B. Wrackmeyer, Multiple receiver experiments for NMR spectroscopy of organosilicon compounds, Appl. Organometal. Chem. 24 (2010) 837–841.
[88] J. Battiste, R.A. Newmark, Applications of ^{19}F Multidimensional NMR, Prog. NMR Spectrosc. 48 (2006) 1–23.
[89] J.-X. Yu, R.R. Hallac, S. Chiguru, R.P. Mason, New frontiers and developing applications in ^{19}F NMR, Prog. NMR Spectrosc. 70 (2013) 25–49.
[90] C. Dalvit, Theoretical analysis of the competition ligand-based NMR experiments and selected applications to fragment screening and binding constant measurements, Concepts in Magn. Reson. 32A (2008) 341–372.
[91] J.L. Kitevski-LeBlanc, R.S. Prosser, Current applications of ^{19}F NMR to studies of protein structure and dynamics, Prog. NMR Spectrosc. 62 (2012) 1–33.
[92] Y.-B. Wan, X.-H. Li, Two-dimensional nuclear magnetic resonance spectroscopy with parallel acquisition of ^{1}H–^{1}H and ^{19}F–^{19}F correlations, Chin. J. Anal. Chem. 43 (2015) 1203–1209.
[93] Ē. Kupče, S. Cheatham, R. Freeman, Two-dimensional spectroscopy with parallel acquisition of ^{1}H–X and ^{19}F–X correlations, Magn. Reson. Chem. 45 (2007) 378–380.
[94] W. Bermel, I. Bertini, I.C. Felli, M. Piccioli, R. Pierattelli, ^{13}C-detected protonless NMR spectroscopy of proteins in solution, Prog. NMR Spectrosc. 48 (2006) 25–45.
[95] L.E. Kay, M. Ikura, R. Tschudin, A. Bax, Three-dimensional triple-resonance NMR spectroscopy of isotopically enriched proteins, J. Magn. Reson. 89 (1990) 496–514.
[96] Ē. Kupče, L.E. Kay, R. Freeman, Detecting the afterglow of ^{13}C NMR in proteins using multiple receivers, J. Am. Chem. Soc. 132 (2010) 18008–18011.
[97] Ē. Kupče, R. Freeman, Projection–reconstruction technique for speeding up multidimensional NMR spectroscopy, J. Am. Chem. Soc. 132 (2010) 18008–18011.
[98] R. Freeman, Ē. Kupče, Distant echoes of the accordion: Reduced dimensionality, GFT-NMR, and projection-reconstruction of multidimensional spectra, Concepts in Magn. Reson. 23A (2008) 63–75.
[99] J.G. Reddy, R.V. Hosur, Parallel acquisition of 3D-HA(CA)NH and 3D-HACACO spectra, J. Biomol. NMR 56 (2013) 77–84.
[100] J.G. Reddy, R.V. Hosur, Complete backbone and DENQ side chain NMR assignments in proteins from a single experiment: implications to structure–function studies, J. Struct. Funct. Genomics 15 (2014) 25–32.
[101] H. Wang, L. Ciobanu, A.S. Edison, A.G. Webb, An eight-coil high-frequency probehead design for high-throughput nuclear magnetic resonance spectroscopy, J. Magn. Reson. 170 (2004) 206–212.
[102] C. Martineau, F. Decker, F. Engelke, F. Taulelle, Parallelizing acquisitions of solid-state NMR spectra with multi-channel probe and multi-receivers: Applications to nanoporous solids, Solid State NMR, Volumes 55–56 (2013) 48–53.
[103] O. Gonen, J. Murphy-Boesch, R. Srinivasan, J.N. Hu, H. Jiang, R. Stoyanova, T.R. Brown, Simultaneous and interleaved multinuclear chemical-shift imaging, a method for concurrent, localized spectroscopy, J. Magn. Reson. 104B (1994) 26–33.
[104] A. Viegas, T. Viennet, T.-Y. Yu, W. Schumann, G. Bermel, M. Etzkorn Wagner, UTOPIA NMR: activating unexploited magnetization using interleaved low-gamma detection, J. Biomol. NMR 64 (2016) 9–15.
[105] Ē. Kupče, R. Freeman, Resolving ambiguities in two-dimensional NMR spectra: the 'TILT' experiment, J. Magn. Reson. 172 (2005) 329–332.
[106] S.M. Pudakalakatti, A. Dubey, G. Jaipuria, U. Shubhashree, S.K. Adiga, D. Moskau, H.S. Atreya, A fast NMR method for resonance assignments: application to metabolomics, J. Biomol. NMR 58 (2014) 165–173.
[107] (a) S.M. Pudakalakatti, A. Dubey, H.S. Atreya, Simultaneous acquisition of three NMR spectra in a single experiment for rapid resonance assignments in metabolomics, J. Chem. Sci., 127 (2015) 1091–1097. (b) J.-N. Dumez, Spatial encoding and spatial selection methods in high-resolution NMR spectroscopy, Prog. NMR Spectrosc., 109 (2018) 101–134.
[108] K.J. Donovan, Ē. Kupče, L. Frydman, Multiple parallel 2D NMR acquisitions in a single scan, Angew. Chem. Int. Ed. 52 (2013) 4152–4155.
[109] P. Giraudeau, Y. Shrot, L. Frydman, Multiple ultrafast, broadband 2D NMR spectra of hyperpolarized natural products, J. Am. Chem. Soc. 131 (2009) 13902–13903.
[110] M. Vega-Vazquez, J.C. Cobas, M. Martin-Pastor, Fast multidimensional localized parallel NMR spectroscopy for the analysis of samples, Magn. Reson. Chem. 48 (2010) 749–752.
[111] T.R. Brown, B.M. Kincaid, K. Ugurbil, NMR chemical shift imaging in three dimensions, Proc. Acad. Natl. Sci. U.S.A. 79 (1982) 3523–3526.
[112] N. Murali, W.M. Miller, B.K. John, D.A. Avizonis, S.H. Smallcombe, Spectral unraveling by space-selective Hadamard spectroscopy, J. Magn. Reson. 179 (2006) 182–189.
[113] C. Herbst, K. Riedel, Y. Ihle, J. Leppert, O. Ohlenschläger, M. Görlach, R. Ramachandran, MAS solid state NMR of RNAs with multiple receivers, J. Biomol. NMR 41 (2008) 121–125.
[114] R. Linser, B. Bardiaux, V. Higman, U. Fink, B. Reif, Structure calculation from unambiguous long-range amide and methyl ^{1}H–^{1}H distance restraints for a microcrystalline protein with MAS solid-state NMR spectroscopy, J. Am. Chem. Soc. 133 (2011) 5905–5912.
[115] A.B. Nielsen, K. Székely, J. Gath, M. Ernst, N.C. Nielsen, B.H. Meier, Simultaneous acquisition of PAR and PAIN spectra, J. Biomol. NMR 52 (2012) 283–288.
[116] J.M. Lamley, J.R. Lewandowski, Simultaneous acquisition of homonuclear and heteronuclear long-distance contacts with time-shared third spin assisted recoupling, J. Magn. Reson. 218 (2012) 30–34.
[117] K. Takeda, Y. Kusakabe, Y. Noda, M. Fukuchi, K. Takegoshi, Homo- and heteronuclear two dimensional covariance solid-state NMR spectroscopy with a dual-receiver system, Phys. Chem. Chem. Phys. 14 (2012) 9715–9721.
[118] K. Sharma, P.K. Madhu, V. Agarwal, K.R. Mote, Unpublished.
[119] M. Bjerring, B. Paaske, H. Oschkinat, Ü. Akbey, N.C. Nielsen, Rapid solid-state NMR of deuterated proteins by interleaved cross-polarization from ^{1}H and ^{2}H nuclei, J. Magn. Reson. 214 (2012) 324–328.

[120] V. Chevelkov, A. Diehl, B. Reif, Measurement of N-15 T1 relaxation rates in a perdeuterated protein by magic angle spinning solid-state nuclear magnetic resonance spectroscopy, J. Chem. Phys. 128 (2008) 52316.
[121] B.-J. van Rossum, F. Castellani, J. Pauli, K. Rehbein, J. Hollander, H.J.M. de Groot, H. Oschkinat, Assignment of amide proton signals by combined evaluation of HN, NN and HNCA MAS-NMR correlation spectra, J. Biomol. NMR 25 (2003) 217–223.
[122] N.J. Traaseth, T. Gopinath, G. Veglia, On the performance of spin diffusion NMR techniques in oriented solids: Prospects for resonance assignments and distance measurements from separated local field experiments, J. Phys. Chem. B 114 (2010) 13872–13880.
[123] K.R. Mote, T. Gopinath, N.J. Traaseth, J. Kitchen, P.L. Gor'kov, W.W. Brey, G. Veglia, Multidimensional oriented solid-state NMR experiments enable the sequential assignment of uniformly ^{15}N labelled integral membrane proteins in magnetically aligned lipid bilayers, J. Biomol. NMR 51 (2011) 339–346.
[124] M.G. Jain, D. Lalli, J. Stanek, C. Gowda, S. Prakash, T.S. Schwarzer, T. Schubeis, K. Castiglione, L.B. Andreas, P.K. Madhu, G. Pintacuda, V. Agarwal, Selective ^{1}H–^{1}H distance restraints in fully protonated proteins by very fast magic angle spinning solid-state NMR, J. Phys. Chem. Lett. 8 (2017) 2399–2405.
[125] K. Sharma, P.K. Madhu, K.R. Mote, A suite of pulse sequences based on multiple sequential acquisitions at one and two radiofrequency channels for solid-state magic-angle spinning NMR studies of proteins, J. Biomol. NMR 65 (2016) 127–141.
[126] N. Ivchenko, C.E. Hughes, M.H. Levitt, Multiplex phase cycling, J. Magn. Reson. 160 (2003) 52–58.
[127] T. Gopinath, G. Veglia, 3D DUMAS: Simultaneous acquisition of three-dimensional magic angle spinning solid-state NMR experiments of proteins, J. Magn. Reson. 220 (2012) 79–84.
[128] C.J. Palmer, B.T. Scott, L.R. Jones, Purification and complete sequence determination of the major plasma membrane substrate for cAMP dependent protein kinase and protein kinase C in myocardium, J. Biol. Chem. 266 (1991) 11126–11130.
[129] T. Gopinath, G. Veglia, Sensitivity enhancement in static solid-state nmr experiments via single and multiple-quantum dipolar coherences, J. Am. Chem. Soc. 131 (2009) 5754–5756.
[130] T. Gopinath, R. Verardi, N.J. Traaseth, G. Veglia, Sensitivity enhancement of separated local field experiments: application to membrane proteins, J. Phys. Chem. B 114 (2010) 5089–5095.
[131] T. Gopinath, G. Veglia, Orphan spin operators enable the acquisition of multiple 2D and 3D magic angle spinning solid-state NMR spectra, J. Chem. Phys. 138 (2013), 184201.
[132] K.R. Mote, T. Gopinath, G. Veglia, Determination of structural topology of a membrane protein in lipid bilayers using polarization optimized experiments (POE) for static and MAS solid state NMR spectroscopy, J. Biomol. NMR 57 (2013) 91–102.
[133] T. Gopinath, G. Veglia, Multiple acquisitions via sequential transfer of orphan spin polarization (MAeSTOSO): How far can we push residual spin polarization in solid-state NMR?, J Magn. Reson. 267 (2016) 1–8.
[134] T. Gopinath, K.R. Mote, G. Veglia, Simultaneous acquisition of 2D and 3D solid-state NMR experiments for sequential assignment of oriented membrane protein samples, J. Biomol. NMR 62 (2015) 53–61.
[135] J.R. Banigan, A. Gayen, N.J. Traaseth, Combination of ^{15}N reverse labelling and afterglow spectroscopy for assigning membrane protein spectra by magic-angle-spinning solid-state NMR: application to the multidrug resistance protein EmrE, J. Biomol. NMR 55 (2013) 391–399.